

**“Mechanisms of assembly and activity-
dependent remodelling of the presynaptic
cytomatrix at the active zone”**

Dissertation
zur Erlangung des akademischen Grades

doctor rerum naturalium
(Dr. rer. nat.)

genehmigt durch die Fakultät für Naturwissenschaften
der Otto-von-Guericke-Universität Magdeburg

von

Dipl. Mol. Biol. Vesna Lazarevic

geb.am

02.06.1978 in Belgrade, Serbia

Gutachter: Prof. Dr. Eckart D. Gundelfinger
Prof. Dr. Susanne Schoch McGovern

eingereicht am: 20.10.2009

vorteidigt am: 04.03.2010

Acknowledgement

The work presented in this dissertation was carried out during the years 2006-2009 in the Department of Neurochemistry and Molecular Biology, Leibniz Institute for Neurobiology, Magdeburg, Germany.

I would like to thank my supervisor Prof. Dr. Eckart D. Gundelfinger for the opportunity to do my doctoral thesis under his guidance.

My special thanks go to Dr. Anna Fejtova for constant support, help and encouragement during my PhD thesis.

Many thanks to Dr. Stefano Romorini and Dr. Wilko Altmann and to all members of Bassoon group (Dasha, Markus, Anne, Alexandra, Diana, Daniela, and Claudia) for fruitful discussions, help and nice atmosphere in the lab. Thank to Cornelia Schoene, former diploma student in our lab, who did all electrophysiology work discussed in the theses.

I would like also to thank Dr. Michael Kreutz, my second supervisor at graduate colleague (GRK1167) and to all scientists from the department for their help during work in the lab and their energy during discussions on seminars.

Many thanks to Dr. Werner Zuschratter and Dr. Karin Richter for help with electron microscopy.

Thanks to Betina, Heidi, Sabine, Janina and Stefi our excellent technicians in the lab who made all the work easier.

Thanks to all current and former colleagues and dear friends from IfN for nice atmosphere at work and nice time that we spend together.

The work presented here was partially supported by GRK1167 and I would like to thank the chairs Prof. Michael Naumann and Prof. Eckart D. Gundelfinger to allowing me to be associated member of GRK. Thanks also to all colleagues from GRK1167 for having nice time at seminars and workshops.

Last but not the least I am very grateful to my family for their love and support.

Vesna Lazarevic

Summary

The release of neurotransmitters is restricted to the specialized region of the presynaptic nerve terminal called the active zone (AZ). At the ultra-structural level, the AZ is characterized as an electron-dense region beneath the presynaptic plasma membrane composed of a meshwork of cytoskeleton and associated proteins, so called, cytomatrix of the AZ (CAZ). To date several CAZ-specific proteins have been characterized: RIMs, Munc13s, ELKS/CAST/ERCs, Bassoon (Bsn) and Piccolo/Aczonin (Pclo).

The first aim of my doctoral thesis was to investigate whether the loss of functional Bassoon and Piccolo may influence assembly, maturation and/or morphological organization of synapses. Since animals double-mutant for both proteins are not viable, we performed an ultra-structural characterization of synapses in primary cultured hippocampal neurons from *Bsn-Pclo* double mutant mice. We could show that synapses are formed in these double-mutant cultures. Comparing the features of the major presynaptic parameters (AZ length, number of synaptic vesicles (SVs), number of docked SVs) between wild-type and *Bsn-Pclo*-double mutant animals, we found that, although two major AZ scaffolding proteins are missing, there is no major difference in the ultra-structure of the presynaptic bouton between these two groups of animals.

As Piccolo and Bassoon are transported to the presynaptic site on specific membrane carriers, the so-called Piccolo-Bassoon transport vesicles (PTVs), we assessed the existence of these 80-nm dense-core organelles in double-mutant cultures. The number of 80-nm dense-core vesicles was found to be significantly reduced suggesting that these AZ precursor vesicles are missing in the absence of Piccolo and Bassoon. Interestingly, the thickness of postsynaptic density (PSD) was significantly reduced. These data suggest that Bassoon and Piccolo are not necessary for synapse formation and assembly, but they have significant role in synapse maturation.

As synapses are complex and highly dynamic structures that are constantly remodelled during development as well as during learning and memory processes, the second aim of my PhD thesis was to investigate whether synaptic activity may alter the molecular composition of the AZ and, if yes, what might be possible molecular mechanisms underlying these activity-dependent changes.

Our experiments revealed that prolonged inhibition of excitatory synaptic transmission (e.g. by blocking ionotropic glutamate receptors) significantly decreases the expression levels of the most CAZ-associated proteins and some of postsynaptic scaffolds, but the expression of SV and SNARE-family proteins was not affected. Also, activity deprivation did not influence the overall number of synapses. Changes in the molecular content of the AZ are reversible within 48 hrs after removal of activity suppressing drugs underpinning the physiological relevance of the observed phenomena. With respect to the mechanisms that governing the activity-dependent remodeling of synapses, we found that inhibition of proteasome-function prevented activity induced decrease of CAZ proteins. This suggests that the ubiquitin-proteasome system might control activity-dependent protein turnover and global compositional changes in the presynaptic AZ. Taken together, our data revealed an unexpected dramatic regulation of CAZ proteins during synaptic plasticity.

Zusammenfassung

Die Freisetzung von Neurotransmittern ist auf eine spezialisierte Region der präsynaptischen Nervenendigung beschränkt, die als aktive Zone bezeichnet wird. Auf ultrastruktureller Ebene wird die aktive Zone durch eine elektronendichte Struktur charakterisiert, die direkt an die präsynaptische Plasmamembran angelagert ist. Sie besteht aus einem Geflecht von cytoskelettalen und damit assoziierten Proteinen, die die so genannte Cytomatrix der aktiven Zone (CAZ) bilden. Bislang sind einige wenige CAZ-spezifische Proteine identifiziert worden. Zu ihnen gehören Mitglieder der Proteinfamilie der RIMs, Munc13, ELKS/CAST/ERCs sowie die Proteine Bassoon(Bsn) und Piccolo/Aczonin (Pclo).

Das erste Ziel meiner Dissertation befasste sich mit der Frage, ob der Verlust von funktionellem Bassoon und Piccolo den Zusammenbau, die Reifung und/oder die morphologische Organisation von Synapsen beeinflussen kann. Da Tiere, bei denen beide Proteine mutiert sind, rasch nach der Geburt sterben, wurde eine ultrastrukturelle Charakterisierung von *Bsn-Pclo*-defizienten Synapsen an hippokampalen Primärkulturen von doppelmutanten Mäusen vorgenommen. Wir konnten zeigen, dass Synapsen in solchen Kulturen gebildet werden. Der Vergleich der präsynaptischen Hauptparameter (Länge der aktiven Zone, Anzahl von synaptischen Vesikeln, Anzahl der gedockten synaptischen Vesikel) zwischen wildtypischen und *Bsn-Pclo*-doppelmutanten Tieren ergab keinen auffälligen Unterschied in der Ultrastruktur der präsynaptischen Endigungen beider Tiergruppen, obgleich zwei Hauptgrundgerüstproteine der aktiven Zone fehlen.

Da Piccolo und Bassoon zu den präsynaptischen Endigungen auf für sie spezifische membranbasierte Transportorganellen, den so genannten Piccolo-Bassoon-Transportvesikeln (PTVs), transportiert werden, wurde der Frage nachgegangen, ob diese 80 nm großen Vesikel mit elektronendichter Füllung (*dense core*-Vesikel) in Doppelmutanten noch existieren. Es stellte sich heraus, dass die Menge an diesen *dense core*-Vesikeln signifikant reduziert ist, was auf einen Verlust dieser Vesikel in Abwesenheit von Piccolo und Bassoon hindeutet. Interessanterweise war die Dicke der postsynaptischen Dichte (PSD), ein elektronendichtes Proteinnetzwerk in der postsynaptischen Endigung, signifikant reduziert. Zusammengefasst lassen diese Daten darauf schließen, dass Bassoon und Piccolo zwar nicht notwendig für die Bildung von Synapsen sind, beide Proteine aber eine signifikante Rolle bei der Reifung von Synapsen besitzen.

Synapsen sind komplexe und hochdynamische Strukturen, die sowohl während der Entwicklung als auch im Verlauf von Lern- und Gedächtnisvorgängen ständig Prozessen der Ummodellierung unterliegen. Das zweite Ziel meiner Arbeit ging daher der Frage nach, inwieweit synaptische Aktivität die molekulare Komposition der aktiven Zone verändert und, wenn ja, welche molekularen Prozesse diesen aktivitätsabhängigen Änderungen zu Grunde liegen.

Unsere Ergebnisse zeigten, dass eine andauernde Inhibition der exzitatorischen Transmission (z.B. durch Blockierung von ionotropen Glutamat-Rezeptoren) zu einer signifikanten Reduktion der Expressionrate der meisten CAZ-assoziierten Proteine führt. Die Expression einiger postsynaptische Gerüstproteine war ebenfalls reduziert, wohingegen die Expression von synaptischen Vesikel-Proteinen und von Mitgliedern der SNARE-Proteinfamilie unverändert blieb. Ebenso hatte die Stilllegung der Aktivität keinen

Einfluss auf die Gesamtzahl an Synapsen. Die Änderungen in der molekularen Zusammensetzung der aktiven Zone waren innerhalb von 48 Stunden nach der Beendigung der aktivitätsblockierenden Behandlung reversibel, was auf eine physiologische Relevanz dieses Phänomens hindeutet. Im Hinblick auf die Mechanismen, die diesen aktivitätsabhängigen Umbau von Synapsen steuern, konnten wir zeigen, dass eine Inhibition der Proteasomen-Funktion eine aktivitätsinduzierte Abnahme an CAZ-Proteinen verhindert. Dies deutet darauf hin, dass das Ubiquitin-Proteasom-System den aktivitätsabhängigen Protein-Umsatz sowie globale Änderungen in der molekularen Zusammensetzung der aktiven Zone kontrollieren könnte. Zusammenfassend weisen unsere Daten auf eine unerwartet starke Regulation von CAZ-Proteinen während synaptischer Plastizität hin.

CONTENTS:

1. INTRODUCTION	1
1.1. The Synapse	1
1.1.1. The architecture of the presynaptic active zone	3
1.1.2. Molecular organization of the presynaptic active zone	4
1.1.3. Cytomatrix at the Active Zone (CAZ)	5
1.1.4. Assembly of the presynaptic active zone – the role of Piccolo-Bassoon transport vesicles (PTVs)	10
1.2. Bassoon and Piccolo mutant mice	12
1.2.1. Bassoon mutant mice	12
1.2.2. Piccolo mutant mice	15
1.3. Activity-dependent remodelling of synapses – Homeostatic plasticity and synaptic scaling	16
1.4. Aims of this work	20
2. MATERIALS AND METHODS	21
2.1. Materials	21
2.1.1. Animals	21
2.1.2. Pharmacological reagents	21
2.1.3. Commonly used buffers	22
2.1.4. Cell cultures	22
2.2. Experimental procedures	23
2.2.1. Genotyping of P0 animals	23
2.2.2. Protein concentration determination: Amidoblack protein assay	24
2.2.3. SDS-PAGE	24
2.2.4. Coomassie staining of SDS-polyacrylamide gels	26
2.2.5. Western blotting	26

2.2.6. Immunoblot detection	26
2.2.7. Immunocytochemistry	27
2.2.8. Electron microscopy (EM)	29
2.3. Data analysis	29
3. RESULTS	30
3.1. Ultrastructural characterization of Bassoon-Piccolo double mutant mice	30
3.2. Activity-dependent remodelling of presynaptic active zone	35
3.2.1. Activity-dependent modulation of synaptic proteins expression level	35
3.2.2. Activity-dependent reduction of CAZ proteins at synaptic sites	38
3.2.3. Prolonged activity deprivation decreases the expression level of synaptic proteins in young cultures	45
3.2.4. Activity-dependent remodeling of the AZ is reversible	47
3.2.5. Activity controls protein degradation	50
4. DISCUSSION	51
4.1. Ultra-structural characterization Bsn-Pclo double mutant mice	51
4.2. Activity dependent remodelling of the AZ	55
4.2.1. Potential role of the ubiquitin-proteasome system in homeostatic plasticity	58
LITERATURE	61
APPENDIX 1	68
Abbreviations	70
Curriculum Vitae	73
Scientific publications	74

Figures and Tables:

Fig. 1. The synapse.	2
Fig. 2. Schematic diagram of interactions of CAZ proteins and the resulting network at the AZ.	5
Fig. 3. Piccolo-Bassoon homology domains.	9
Fig. 4. The active zone transport vesicle hypothesis.	11
Fig. 5. Bassoon mutant mice.	12
Fig. 6. Piccolo mutant mice.	15
Fig. 7. Expression loci of synaptic homeostasis at central synapses.	18
Fig. 8. Basson -Piccolo double mutant mice.	30
Fig. 9. Staining of the cultured hippocampal neurons from WT and Bsn-Pclo double mutant mice for synaptic proteins.	31
Fig. 10. Parameters that morphologically define the synapses.	32
Fig. 11. The ultra-structure of synapses from hippocampal neurons.	33
Fig. 12. Experimental setup.	35
Fig.13. Synaptic activity regulates the composition of CAZ and PSD.	37
Fig.14. Overall number of synapses revealed by Synaptophysin staining was unchanged upon synaptic network activity deprivation.	38
Fig.15. Prolonged synaptic network inhibition did not alter the amount of SV proteins.	39
Fig. 16. Activity-dependent reduction of CAZ proteins at synaptic sites.	42
Fig. 17. Activity-dependent reduction of the postsynaptic scaffold protein Homer1.	43
Fig. 18. No activity-dependent changes in the number of voltage-dependent Ca ²⁺ channels.	44
Fig. 19. Prolonged activity blockade increases the number of VGLUT1 positive puncta per 20 microns of dendrite.	44
Fig. 20. Prolonged activity deprivation decreases the expression level of synaptic proteins in young cultures (15 DIV).	46
Fig. 21. Immunoblot analysis of synaptic proteins 24hrs after synaptic network deprivation (APV/CNQX) or activity enhancement (PTX).	47
Fig. 22. Scheme of the four experimental groups to test the reversibility of drug treatment.	48
Fig. 23. Activity dependent reduction in the expression level of CAZ-specific proteins is reversible.	48

Fig. 24. Activity dependent down-regulation of selected synaptic proteins is reversible.	49
Fig. 25. Activity dependent reduction in the expression level of CAZ-specific proteins upon activity blockade can be rescued by proteasome blockade.	50
Fig. 26. Model of excitatory central synapse formation.	53
Supplementary Fig. S1.	68
Supplementary Fig. S2.	68
Supplementary Fig. S3.	69
Table 1. Animal lines.	21
Table 2. Pharmacological reagents.	21
Table 3. Commonly used buffers.	22
Table 4. Cell culture media.	22
Table 5. Solutions for DNA extraction, agarose gel electrophoresis.	23
Table 6. Primer sequences for genotyping.	23
Table 7. PCR program for genotyping.	23
Table 8. Solutions for Amidoblack protein assay.	24
Table 9. Laemmli system.	25
Table 10. SDS-PAGE under reducing conditions by the Tris-acetate system.	25
Table 11. Solutions for Coomassie staining.	26
Table 12. Blotting buffers.	26
Table 13. Primary antibodies for Western blot and Immunostaining.	28
Table 14. Secondary antibodies for Western blot and Immunostaining.	28
Table 15. Morphometric analysis of synapses in cultured hippocampal neurons of WT and Bassoon-Piccolo double mutant mice.	33
Table 16. Percent change (relative to control) in synaptic protein levels 48hrs after adding PTX or APV/CNQX.	36
Table 17. APV/CNQX treatment reduces the levels of CAZ and PSD proteins in synapses.	40
Table 18. Percent change in protein levels after adding of APV/CNQX for 48hrs and recovery of the protein expression level 48 hrs after removing the drug.	49

1. INTRODUCTION

1.1. The Synapse

Chemical synapses are functional connections between neuronal cells in the brain. The human brain contains about 10^{15} synaptic contacts, connecting 10^{10} - 10^{11} neurons. They are crucial for the interneuronal signaling required for the processing and integration of information during development, learning and memory formation. Synapses are composed of three compartments: presynaptic bouton, synaptic cleft and postsynaptic part containing postsynaptic reception apparatus.

The presynaptic terminal (also called presynaptic bouton) contains clear, 40-50 nm diameter vesicles, named synaptic vesicles (SV) where neurotransmitters are stored. The release of neurotransmitters is restricted to a specialized region of the presynaptic bouton, called, the active zone (AZ). Typically, a presynaptic bouton contains hundreds of vesicles that are clustered in close proximity of the AZ. However, it is thought that not all SVs in the presynaptic terminal are functionally identical. They seem to belong to different pools of vesicles, i.e., either to the reserve (also called the resting) pool or to the recycling pool of SVs (reviewed in Gundelfinger et al., 2003). A subpopulation of the vesicles of the recycling pool is tethered to the presynaptic plasma membrane and primed for the fusion step (i.e. the readily releasable pool, RRP) (Fig.1.). In response to action potentials (AP) arriving in the presynapse and increased levels of Ca^{2+} ions in the nerve terminal, the SV membrane fuses with the presynaptic plasma membrane and neurotransmitters are rapidly released into the about 20 nm wide space between the membranes of the pre- and the post-synaptic cell, called synaptic cleft. Discharged neurotransmitter molecules then diffuse across the cleft and activate receptors in the postsynaptic membrane thus signaling can be further transmitted to downstream target cells. In general, neurotransmission can be excitatory or inhibitory, depending of the type of neurotransmitters that are released from the presynapse and, on the postsynaptic receptors that are activated upon their release. The majority of the excitatory synaptic transmission in the mammalian brain is mediated by the neurotransmitter glutamate, and there are two major pharmacologically distinct classes of ionotropic glutamate receptors: the NMDA (N-methyl-D-aspartate) receptors and AMPA (α -amino-3-hydroxy-5-methylisoxazole-4-propionic acid) receptors. AMPA receptors mediate rapid synaptic transmission whereas NMDA receptors are important in the activity-dependent synaptic plasticity which underlies learning and memory (reviewed in Kim J.H. & Huganir R., 1999).

GABA (gamma-aminobutyric-acid) is an inhibitory neurotransmitter which activates inhibitory GABAergic receptors (GABA_A and GABA_B receptors).

The receptors are incorporated into the postsynaptic membrane. Their proper localization and function is organized by a variety of the postsynaptic proteins, referred as PSD proteins (PSD, postsynaptic density), as they can be observed under electron microscope (EM) as electron-dense material beneath the postsynaptic membrane. Studies on biochemically isolated PSDs revealed that, apart from the receptors, the major constituents of the PSD at excitatory synapses include cytoskeletal proteins (actin, tubulin, fodrin), signalling molecules (CaMKII, calmodulin) and scaffolding proteins (PSD-95, Homer, Shank/ProSAPs, GKAP/SAPAP etc.) (reviewed by Okabe., 2007).

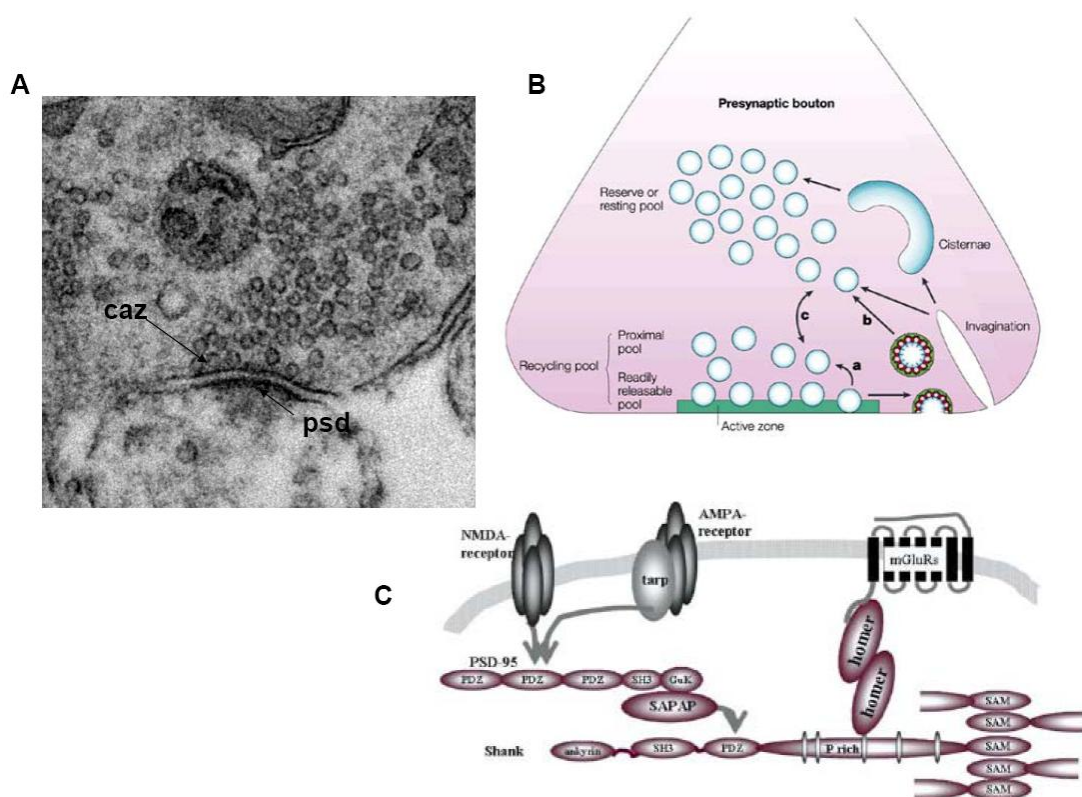


Fig. 1. The synapse. (A) Electron micrograph of the central synapse (V. Lazarevic, unpublished). Electron-dense material might be observed at both, presynaptic (CAZ, Cytomatrix at the Active Zone) and postsynaptic site (PSD, postsynaptic density). (B) Distinct synaptic vesicle pools in presynaptic bouton (reviewed in Gundelfinger et al., 2003). (C) Integration of the glutamatergic receptors through Shank and the attached postsynaptic proteins PSD-95, Homer and SAPAP (reviewed in Kreienkamp, 2008).

Upon stimulation of the nerve terminal by depolarizing axon potentials the SV membrane is incorporated into the plasma membrane by exocytosis and then needs to be retrieved by the compensatory mechanism, called endocytosis. Both, exo- and endocytosis, are part of the SV cycle and have to be coordinated in a very efficient way to ensure proper signal transduction from the presynaptic to the postsynaptic neuron. It is

believed that a meshwork of cytoskeletal and associated proteins, called cytomatrix of the AZ (CAZ), plays a key role in the spatial and temporal coordination of the SV cycle. Under the electron microscope (EM), the CAZ can be observed as electron-dense material that is adjacent to the presynaptic membrane (Fig. 1). To date, only a few CAZ-specific proteins, including RIMs, Munc13, CAST/ERCs, Bassoon and Piccolo/Aczonin have been characterized. During recent years, a lot of efforts have been made to highlight the contribution of these proteins in the coordination and modulation of exo- and endocytosis, as well as, to elucidate their role in synapse assembly, maturation and remodelling during development and plasticity processes such as learning and memory formation.

1.1.1. The architecture of the presynaptic active zone

The AZ in the presynaptic nerve terminal is a highly organized, complexly designed and dynamic structure. Although the morphology of the AZs and the molecular composition might vary among species, tissues and cells, their architectural design seems to be conserved. All AZs consist of three morphologically and functionally distinct components: (1) the plasma membrane of the AZ where SVs fuse; (2) the cytomatrix associated with the plasma membrane where SVs are docked, and (3) electron-dense projections extending from the cytomatrix into the cytoplasm on which SVs are tethered (Zhai and Bellen, 2004)

The plasma membrane of the AZ is precisely aligned with the PSD and its primary function during neurotransmitter release is to mediate fusion of the SVs upon Ca^{2+} entry. This is achieved by localization of the SVs fusion machinery (SNARE complex) in the close proximity of the voltage-gated Ca^{2+} channels.

In the electron microscope, the cytomatrix underlying the AZ plasma membrane and projections extending from the cytomatrix are displayed as an electron-dense web-like network with docked SVs nested between them. The electron-dense nature of this cytomatrix suggests that a large number of proteins is densely packed there (cytoskeletal proteins, presynaptic scaffolds and CAZ-specific proteins). Dense projections extending from the cytomatrix of the AZ might have different size and shape in different types of the synapses, but their main function might be to tether SVs. At the *Drosophila* neuromuscular junctions (NMJs) there are T-shaped dense projections, called T-bars. In vertebrate sensory synapses involved in vision, hearing and balance specialized projections are called synaptic ribbons.

More recently, an elegant study using electron tomography combined with high-pressure freezing without aldehyde fixative has provided the first three-dimensional views

of the presynaptic terminal cytomatrix (Siksou et al., 2007). This study revealed that SVs are interconnected via a dense meshwork of the filaments: one kind of 30-60nm in lengths might represent Synapsin molecules and longer ones (~60nm) that are connecting SVs to the AZ plasma membrane. They might represent CAZ proteins, but currently their real nature is unclear. It is just known that these filaments are more abundant at the AZ than extra-synaptically and they could anchor the network of the bridged SVs in front of the AZ.

1.1.2. Molecular organization of the presynaptic active zone

To ensure proper neurotransmission AZs possess unique structural and functional specializations that are not seen in other secretory systems (Rosenmund et al., 2003.). First, it is known that neurotransmission is a very fast process, meaning that the AZs have to be specialized for temporal coordination of synaptic inputs (action potential) and neurotransmitter release. Second, for direct and accurate signal propagation in neuronal network it is important that the release of neurotransmitters is spatially restricted to the area of the AZ, which typically has a diameter of 200-300 nm. And third, an important feature of the AZ is the dynamic regulation of the overall efficiency and reliability of the transmitter release. Over the past decades, a number of proteins and protein families have been identified that are important for AZ assembly and function. The core molecular structure of the AZ is made by CAZ proteins, but there are also a variety of the proteins that are associated with the CAZ, the occurrence of which is not restricted to the AZ. These proteins include: 1) SV proteins and proteins involved in SV fusion, like SV2, synaptotagmins, SNARE-proteins, syntaxins, Munc18; 2) the cytoskeletal proteins actin, tubulin, myosin; 3) presynaptic scaffolds, such as, synapsins, CASK, Mint; 4) voltage-dependent Ca^{2+} -channels; and 5) cell adhesion molecules, e.g. neurorexins, cadherins, integrins (Schoch & Gundelfinger, 2006) (Fig. 2)

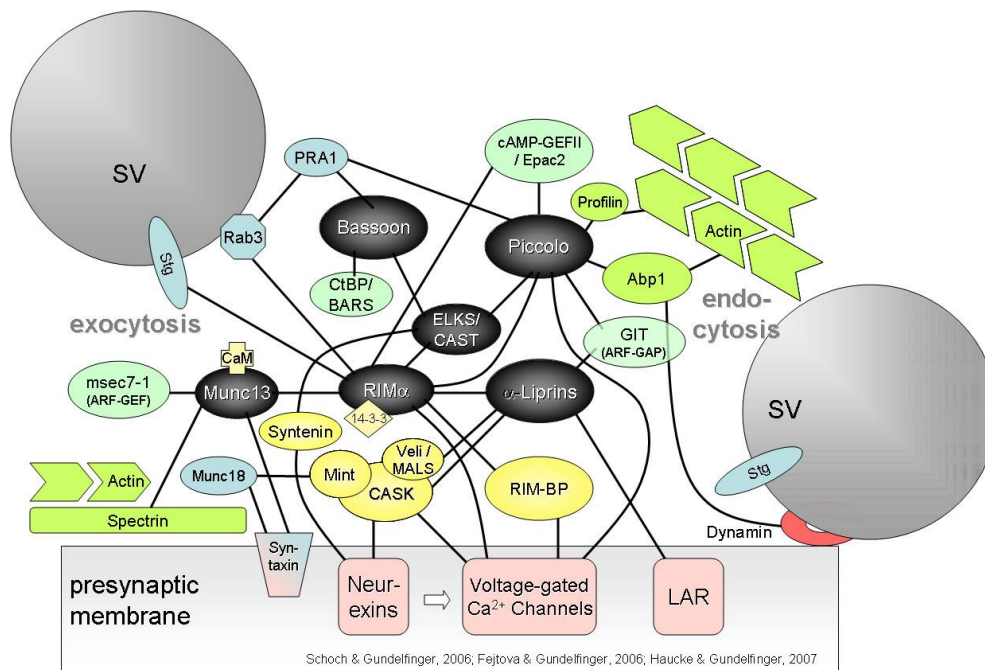


Fig. 2. Schematic diagram of interactions of CAZ proteins (in black) and the resulting network at the AZ (modified from Schoch and Gundelfinger, 2006)

1.1.3. Cytomatrix at the Active Zone (CAZ)

As mentioned above, the spatial and temporal organization of SV cycle is a tightly controlled process coordinated by a CAZ protein network. To date, five CAZ-specific protein families have been characterized: Bassoon, Piccolo/Aczonin, RIMs, Munc13s, ELKS/CAST/ERC proteins and Liprin- α proteins. It is believed, that these multi-domain proteins form a scaffold at the AZ through their physical interactions and play a role not only in organization of the exo- and endocytotic processes, but also in synapse assembly and maturation, and in the regulation of the neurotransmitter release during synaptic plasticity.

Munc13 proteins

Munc13 proteins constitute a family of three highly homologous molecules (Munc13-1, Munc13-2 and Munc13-3.) and with the exception of the ubiquitously expressed Munc13-2 all other Munc13s are brain-specific and preferentially localized to presynaptic terminals. Immunoelectron microscopic data have demonstrated that Munc13-1 is highly enriched in presynaptic AZ (Betz et al., 1998). The key role of Munc13 proteins is SVs priming. SVs that are docked to the plasma membrane at the site of release have to be primed to a fusion competence. Fusion of SVs with the plasma membrane requires the formation of the SNARE (soluble N-ethylmaleimid-sensitive factor attachment protein

receptor) complex and Munc13 proteins are thought to facilitate SNARE complex assembly by inducing a conformational switch in Syntaxin from a “closed” to an “open” conformation or, by providing a template for the assembly of Syntaxin1/SNAP-25 heterodimers (reviewed by Rizo & Rosenmund, 2008.). Munc13-mediated SV priming is absolutely essential for SV fusion as illustrated by the total abrogation of the spontaneous and evoked release in the hippocampal neurons of Munc13-1/2 double knockout mice (Varoqueaux et al., 2002.). Recently, high-pressure freezing combined with electron tomography was used for the ultrastructural characterization of the synapses from Munc13-deficient mice (Siksou et al., 2009). The authors could show that in mutant mice, SVs are not docked to the plasma membrane of the AZ, but remain at the short distance from the membrane. These findings suggest that SVs docking and priming are morphological and physiological manifestations of the same molecular process that is mediated by both, SNARE complexes and Munc13 proteins.

RIM proteins

RIM (Rab3-interactions molecule) proteins have been initially discovered by Wang et al. (1997) as putative effectors for the small SV-binding protein Rab3 which is important for the SV fusion during exocytosis. In vertebrates, there are 4 RIM genes that encode six principal isoforms (RIM1 α , RIM2 α , RIM2 β , RIM2 γ , RIM3 γ , RIM4 γ). As shown in Fig. 2, RIMs might interact with multiple synaptic proteins, such as, Munc13, Bassoon, ELKS/CAST/ERC, Liprins, voltage-gated Ca²⁺ channels, 14-3-3 adaptor proteins etc. Munc13-1/RIM1 interaction is essential for a step in the SV cycle that precedes vesicle fusion (Betz et al., 2001). Similar to the total loss of Munc13-1, disruption of this interaction in wild-type hippocampal neurons leads to a drastically reduced primed and readily releasable pool of vesicles, which in turn, causes a strong reduction in evoked release. One of the possible molecular mechanisms underlying this process could be through the formation of the tripartite complex, Rab3-RIM-Munc13, that would bring SVs in the close proximity to the priming machinery. Analyzing RIM1 α knockout mice revealed that this protein also has the important role during priming and post-priming steps related to calcium-triggered vesicle fusion (Calakos et al., 2004.). Deletion of RIM1 α is not lethal and RIM1 α deficient synapses do not exhibit major ultrastructural alternations suggesting that this protein probably is either complemented by another family member or not involved in SV docking or in the assembly of the AZ as such. On the other hand, RIM1 α deficiency causes a large reduction in the readily releasable pool of vesicles (by 50%, correlating with the 50% decrease of Munc13-1 observed in the brain of these mice) and changes the properties of evoked asynchronous release. Moreover, the Rab3A-RIM1

pathway was also identified as a key player in presynaptic LTP. Lonart et al. (2003) found that PKA phosphorylation of RIM1 α triggers presynaptic LTP at cerebellar parallel fibre synapses. Behavioral studies showed that RIM1 α might be critical for normal learning and memory formation (Powell et al. 2004).

ELKS/CAST/ERC proteins

The name ELKS was given to these proteins according to high content of the amino acids glutamate (E), leucine (L), lysine (K) and serine (S), but since they were isolated independently in two different screens, where they were also named ERCs (Wang et al., 2002) or CASTs (CAZ-associated structural protein; Ohtsuka et al., 2002). In mammals, there are two ELKS genes encoding for two homologous ELKS proteins: ELKS1, also known as ERC1/CAST2; and ELKS2 (ERC2/CAST). Alternative splicing of the ELKS1 transcript produces two isoforms (ELKS1A and ELKS1B) with the different tissue distributions and biochemical properties. ELKS1B and ELKS2 are brain-specific and ELKS1A is primarily synthesized outside the brain. Also, it was shown that ELKS2 is specifically localized to the AZ whereas ELKS1B is present in both, AZ and cytoplasm (reviewed in Schoch & Gundelfinger, 2006.). The exact role of these proteins in mammals is not known, but it has been shown that they can form large molecular complexes with other CAZ proteins (RIMs, Bassoon, Piccolo, Liprin- α). Binding of ELKS to RIM1 is necessary for the proper localization of the RIM at the AZ (Ohtsuka et al., 2002). Since RIM1 is a target for the small SV-binding protein, Rab3, and also interacts with Munc13 it is believed that this complex might control recruitment of SVs and regulate their subsequent fusion with the presynaptic plasma membrane. In addition, it was shown that interfering with ELKS binding to RIM and Bassoon might diminish synaptic transmission (Takao-Rikitsu et al., 2004). The *Drosophila* homologue of ELKS is called Bruchpilot (BRP) and is important for the assembly of T-bars and correct localization of the AZ components in neuromuscular synapses (Kittel et al., 2006). Recently, Fouquet et al (2009) identified BRP as an integral T-bar component responsible for the effective clustering of Ca²⁺-channels during AZ maturation. The other AZ-organizing protein in *Drosophila*, DLiprin- α , (see below) enters nascent AZs substantially earlier than BRP. According to this, the emergence of presynaptic dense bodies (T-bars), which are involved in clustering Ca²⁺-channels, represent the central aspect of synapse maturation in *Drosophila*. Whether similar mechanisms operate during synapse formation and maturation in mammals remains an open question.

Liprin- α proteins

The Liprin- α family of proteins was first identified by their interaction with the LAR-RPTPs (LAR family of receptor protein tyrosine phosphatases) (Serra-Pages et al., 1995). In vertebrates, four liprin- α genes were found, liprin- α 1, α 2, α 3 and α 4, whereas *C. elegans* and *Drosophila* have only a single liprin- α gene: *syd-2* (synapse-defective-2) and D-liprin. Liprin- α 2 and liprin- α 3 are expressed primarily in mammalian brain, while liprin- α 1 and liprin- α 4 are also found in non-neuronal tissues. Liprin- α proteins are well conserved with ~50% amino acid identity between human liprin- α 1 and worm SYD-2. To date Liprin- α proteins have been implicated in multiple processes important for proper cellular and synaptic function (Spangler and Hoogenraad, 2007). In immature neurons, liprin- α proteins are necessary for presynaptic development. Analyzing the SYD-2 mutants (a loss-of-function mutant of the *C. elegans*) revealed that its absence causes a variety of structural presynaptic defects. AZs in these mutants were lengthened and SV proteins were diffusely localized rather than clustered at presynaptic sites, implying that SYD-2 protein is specifically responsible for the recruitment of synaptic proteins. *Drosophila* Dliprin- α mutants display a similar defect in active zone morphology, an increase in the synapse size and abnormal AZ structure. Liprin- α proteins are also important for normal neurotransmitter release as shown that, in both of the above-described invertebrate mutants, synaptic transmission was impaired. In mammals, liprin- α proteins associate with two major synaptic protein complexes that have been closely linked to presynaptic neurotransmitter release and vesicle cycling: ELKS (CAST/ERCs) and RIM. Binding to the RIMs is thought to link RIM-containing active zones to Rab3A-positive synaptic vesicles. In addition the interaction of the Liprin- α is with the MALS (mammalian LIN-seven protein) – CASK (Ca²⁺/calmodulin-dependent serine protein kinase) – Mint1 complex seems to be important. It is believed that both these presynaptic Liprin- α complexes might be involved in recruiting components of the synaptic release machinery to the AZ and thereby facilitating neurotransmitter release. Furthermore, it was also shown that Liprin- α proteins are involved in multiple processes related to the postsynaptic development, e.g. via interaction with the glutamate receptor interacting protein GRIP (Wyszynski et al. 2002), and in intracellular trafficking via their interactions with the motor protein KIF1A (Shin et al. 2003)).

Bassoon and Piccolo/Aczonin

Bassoon (tom Dieck et al., 1998) and Piccolo/Aczonin (Cases-Langhoff et al., 1996; Fenster et al., 2000; Wang et al., 1999) are structurally related and the largest known CAZ-specific proteins (420 and 530 kDa, respectively). They are present in both,

excitatory and inhibitory synapses of all brain regions, but especially abundant in hippocampus, cerebellum and cortex (Richter et al., 1999). Both proteins share 10 regions of high sequence homology, called Piccolo-Bassoon homology domains (PBH) (Fig. 3).

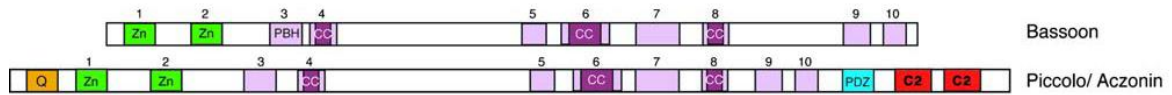


Fig. 3. Piccolo-Bassoon homology domains. Bassoon and Piccolo are structurally related proteins composed of two zinc finger domains (Zn1, Zn2), three coiled-coil domains (CC), several proline-rich sequences (e.g. Q in Piccolo), and 10 regions of homology called Piccolo-Bassoon homology domains (PBH1–10) (adopted from Schoch & Gundelfinger, 2006).

The functions of Bassoon and Piccolo are not fully clarified. Their multi-domain structure and large size suggest that these proteins can act as major scaffolding proteins of the CAZ. Moreover, they are among the earliest proteins incorporated into nascent synapses during synaptogenesis suggesting a possible role for them in the assembly of the AZ (Zhai et al., 2000). Through the interaction with the CAZ protein ELKS (Takao-Rikitsu et al., 2004) they might be involved in AZ organization and neurotransmitter release. In the mouse retina, Bassoon directly binds and functionally interacts with the CtBP-family member, RIBEYE, the protein postulated to serve as a central building block of synaptic ribbons (Schmitz et al., 2000; tom Dieck et al., 2005). In Bassoon-deficient mice, due to the loss of this interaction, photoreceptor ribbons are not anchored at the presynaptic AZ, but float freely at the cytoplasm (Dick et al., 2003). Piccolo might interact with SV-associated protein PRA1 taking a role in the trafficking of the SVs at the AZ (Fenster et al., 2000) and through the interaction with Actin/Dynamin-binding protein Abp1, it might act as a link between the dynamic actin cytoskeleton and SV recycling (Fenster et al., 2003). Using RNA interference to eliminate Piccolo expression, Leal-Ortiz et al. (2008) could show that, although Piccolo is not required for synapse formation, it does influence presynaptic function by modulation of Synapsin1a dynamics in presynaptic bouton. More recently, Fejtova et al (2009) reported the direct interaction of Bassoon with Dynein light chains (DLCs) through which Bassoon may function as a cargo adapter for retrograde axonal transport. In this study, we showed that disruption of the Bassoon-DLC interactions leads to impaired trafficking of Bassoon in neurons and affects the distribution of both Bassoon and Piccolo among synapses. Taken together, all data support the view that Bassoon and Piccolo play an important role in synapse assembly, maturation and function.

1.1.4. Assembly of the presynaptic active zone – the role of Piccolo-Bassoon transport vesicles (PTVs)

The mechanisms of synaptogenesis in the CNS are under intense research. Cell-cell contacts initiated by filopodia are thought to play a central role in inducing synapse formation, but what signals promote filopodia formation, which key adhesion molecules are involved in this process and what presynaptic and postsynaptic cascades are triggered by these adhesion-induced events is still largely unknown.

However, it has been shown that synapse assembly occurs already 1 to 2 hrs after the initial axo-dendritic contact and, interestingly, it seems that presynaptic active zone may become functionally active prior to the maturation of the postsynaptic reception apparatus (Vardinon-Friedman et al., 2000). This momentum of synapse formation could be achieved by a rapid recruitment of pre-assembled synaptic components to the sites of cell-cell contact.

A study performed by Ahmari et al., (2000) showed that at sites of newly forming synapses some clusters of vesicles containing synaptic proteins can be found. Further analysis of synaptogenesis in cultured hippocampal neurons has revealed that major scaffolds of the AZ, Bassoon and Piccolo, are expressed during early stages of neuronal differentiation, and in axons of immature neurons they are specifically associated with a class of 80 nm dense-core vesicles, which have been termed Piccolo-Bassoon transport vesicles (PTVs) (Zhai et al., 2001; Shapira et al., 2003). Interestingly, a variety of additional molecules, including RIMs, Syntaxin, SNAP25 and N-cadherin were also found on these vesicles, but not SV proteins like VAMP2/Synaptobrevin, Synaptophysin or Synaptotagmin.

Based on our current knowledge it is hypothesised that PTVs may represent AZ precursor vesicles. During development these precursor vesicles transport AZ components into nascent synapses, providing scaffolds for the recruitment of the exocytic apparatus including SVs. Time-lapse imaging showed that PTVs are highly mobile entities and quantitative analysis of their content reveals that 2-3 PTVs are necessary to be inserted into presynaptic plasma membrane to form functional AZ (Shapira et al., 2003). More recently, Dresbach et al. (2006) showed that both, Bassoon and Piccolo co-localize with markers of the trans-Golgi network, suggesting that association of PTVs with trans-Golgi compartment is an obligatory step in transport of presynaptic cytomatrix proteins to the synapse (Fig. 4).

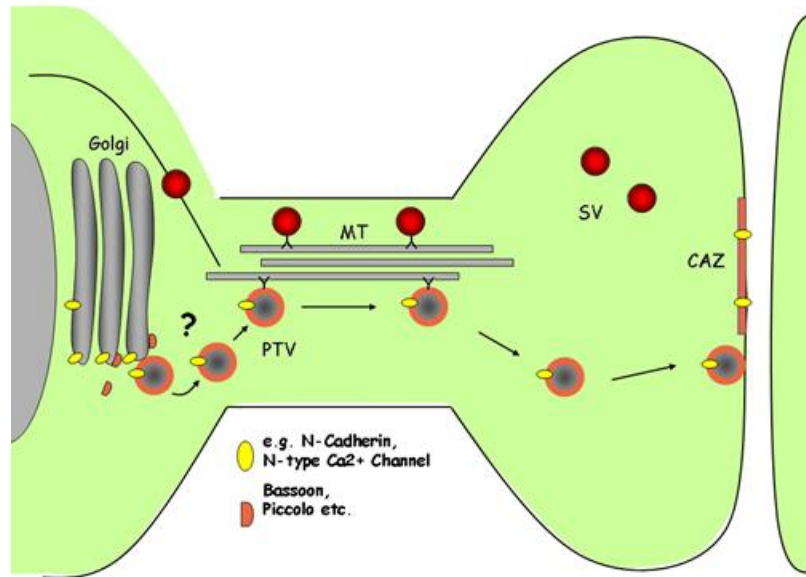


Fig. 4. The active zone transport vesicle hypothesis (modified from Dresbach et al. 2003). During brain development the active zones are pre-assembled in neuronal cell bodies. They are transported along the axons as so-called Piccolo-Bassoon transport vesicles (PTVs) to sites of synaptogenesis where can fuse with the presynaptic plasma membrane and form functional synapse.

1.2. Bassoon and Piccolo mutant mice

1.2.1. Bassoon mutant mice

To establish the role of Bassoon in the assembly and functional organization of the AZ, mutant mice lacking the central region of the Bassoon protein were generated by Altmann et al., (2003). In these *Bsn*-mutant mice, exons 4 and 5 of the *Bsn* gene are not expressed removing the amino acids 505 to 2889 from Bassoon protein (the C-terminal half of the second zinc finger to a region N-terminal of the third CC domain of wild-type *Bsn*). These mice still express a 180-kDa mutant protein, which is not present in wild type animals and which is encoded by 9-kb transcript resulting from joining exons 3 and 6 (Fig. 5).

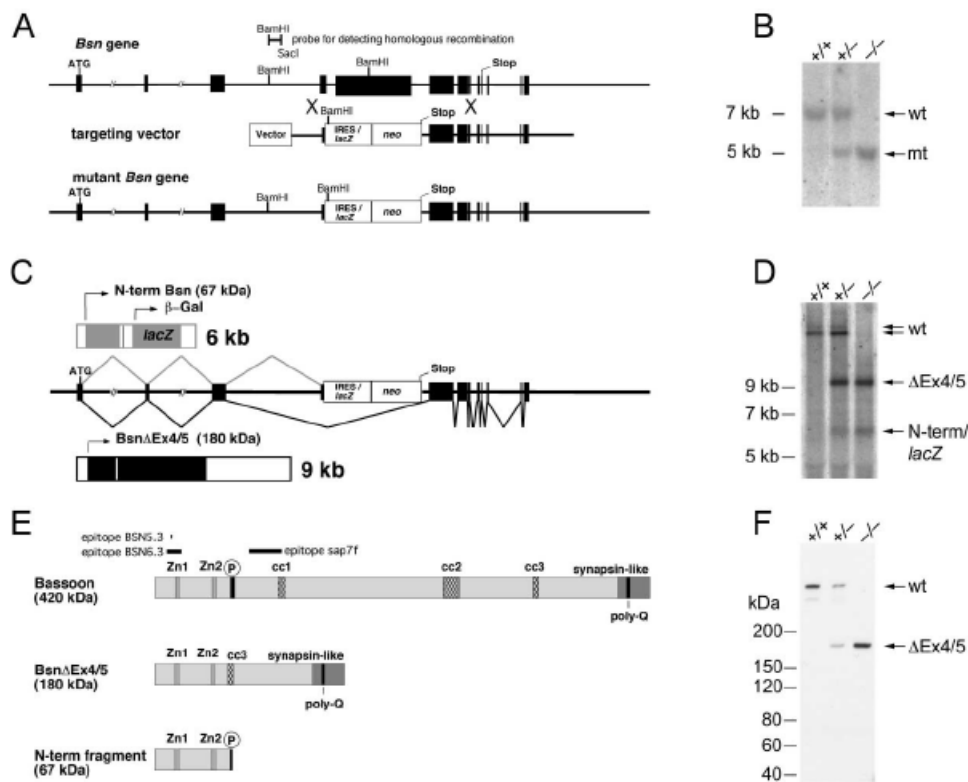


Fig. 5. Bassoon mutant mice. Targeted disruption of the Bassoon gene and analysis of transcript and protein expression in Bassoon mutant mice (Altmann et al., 2003).

(A) Maps of the Bassoon gene, the targeting vector and the resulting mutant gene. (B) Southern blot analysis of genomic DNA of WT (+/+), heterozygous (+/-) and homozygous mutant (-/-) mice. (C) Alternative splicing of the mutant allele results in two transcripts. The 6kb transcript encodes the N-terminal 67 kDa fragment of Bassoon and β -galactosidase. In frame splicing from exon 3 to exon 6 gives rise to a 9 kb transcript encoding *Bsn* Δ Ex4/5. (D) Northern analysis of brain RNA reveals two transcripts (>13kb) in WT mice, the two transcripts depicted in (C) in -/- mutants, and all four transcripts in +/- mice. Blots were hybridized with an exon 2 probe. (E) Schematic representation of Bassoon proteins derived from WT and mutant transcripts. (F) Immunoblot analysis of brain homogenate from +/+, +/- and -/- mice.

Mutant Bassoon is more diffusely distributed in comparison with WT protein and unlike WT-Bsn, it does not co-localize with Piccolo in cultured hippocampal neurons. Biochemical data revealed that in comparison to WT protein, which co-purifies with synaptic junctions, the mutant 180-kDa Bassoon is not enriched in this fraction, but a large fraction is found in the cytoplasmic protein fraction. These findings suggest that the central part of Bassoon, which is absent in mutant protein, is responsible for its anchoring to the AZ and tight association with CAZ. Consistently the region for efficient synaptic targeting of Bassoon via the trans-Golgi network has been localized within this central region (Dresbach et al., 2003). Interestingly, the loss of WT Bassoon did not influence synaptic localization or expression level of other CAZ-specific proteins (RIMs or Munc13s) but did influence the expression level of related protein Piccolo, which is up-regulated 1.4-fold in Bassoon mutant mice.

Bassoon-mutant mice are viable and normal at the birth, but 50% of the homozygous animals die during the first 6 months of life due to rapidly generalizing epileptic seizures. Electrophysiological recordings revealed that the loss of functional Bassoon causes a reduction in normal synaptic transmission due to inactivation of a significant fraction of excitatory synapses (Altrock et al., 2003). At these synapses, SVs are clustered and docked in normal numbers but they are unable to fuse. Although Bassoon is thought to be one of the major presynaptic scaffolds, loss of its function did not alter synapse morphology. It has been shown that, at the ultra-structural level, conventional synapses of Bassoon-mutant mice appear normal concerning the length of the AZ, number of docked SVs or SVs density. Characterization of the brain architecture in mice lacking functional Bassoon (Angenstein et al. 2007) showed a significant increase in the total brain volume, mainly caused by changes in cortex and hippocampus. More recently, interesting studies by Ghiglieri et al., (2009), on Bassoon-mutant mice concerning the epilepsy-induced changes in striatal synaptic plasticity revealed that mutant mice exerted reduced long-term potentiation in striatal spiny neurons, alternations in their dendritic morphology and higher number of fast-spiking interneurons. Using a biochemical approach, the authors showed an altered NMDA receptor subunit composition in mutant animals (a significant increase in NR2A and decrease in NR2B subunit of NMDA receptors). Interestingly, chronic antiepileptic treatment of mutant animals with valproic acid did not only reduce the epileptic seizures, but also normalized synaptic plasticity and NMDA subunit composition in these mice. Taken together, this study revealed new insights into previously described electrophysiological and molecular alternations in mutants, suggesting that the observed changes probably are not all induced directly by the lack of functional Bassoon, but most could be a consequence of the seizure activity. On the other hand, anti-epileptic treatment failed to reverse

morphological alternations in Bassoon mutant mice, meaning, that these changes might represent a direct effect of the lacking of functional Bassoon.

As Bassoon is highly expressed in the rodent retina, Dick et al. (2003) used the same mouse model to investigate the role of Bassoon in ribbon synapse formation. The ribbon is a structurally and functionally specialized type of presynaptic AZ in retinal photoreceptors, and it is actually thought that the synaptic ribbon is an equivalent to the CAZ of conventional synapses (Zhai & Bellen, 2004; tom Dieck et al., 2005). Analyzing the retinas from Bassoon-deficient mice the authors found that retinal anatomy remained unaffected, but the mutation of Bassoon prevented the anchoring of the synaptic ribbon to the presynaptic active of the photoreceptor cell. This resulted in impaired photoreceptor synaptic transmission, altered differentiation of dendrites of postsynaptic neurons and formation of ectopic synapses. Ribbon synapses are also present in cochlear inner hair cells (IHCs) and it has been shown that in Bassoon-mutant mice anchoring of IHC ribbons are largely impaired causing disturbed synchronous auditory signaling. In these mice, a dramatic shift in the threshold of sound detection has been observed (Khimich et al., 2005).

Taken together, these studies suggest that Bassoon plays an important role in assembling and functioning of various types of synapses.

1.2.2. Piccolo mutant mice

In Piccolo-mutant mice the first C2 domain is deleted, resulting in the down-regulation of both, Piccolo transcript and protein product, presumably due to impaired transcript stability (T. Südhof, personal communication). Western blot analysis showed that mutant mice still express truncated mutant protein at about 6% of WT Piccolo levels (A. Fejtova, personal communication; Fig. 6.). Piccolo mutants are viable but often smaller than WT littermates, possibly due to impaired endocrine secretion of insulin or growth hormones. A detailed characterization of this phenotype is still in progress.

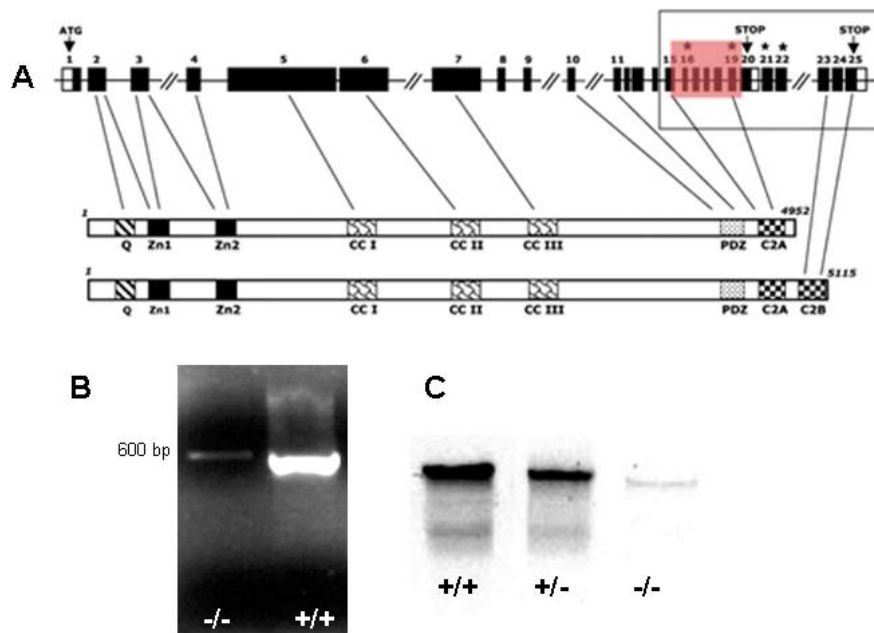


Fig. 6. Piccolo mutant mice. (A) The map of the Piccolo gene with targeted deletion of the first C2 domain (red square). (B) RT-PCR from *Pclo* mutant mice (-/-) and WT animals (+/+) and (C) corresponding Western blots from WT (+/+), heterozygote (+/-) and mutant mice (-/-). Figure by courtesy of A. Fejtova.

1.3. Activity-dependent remodelling of synapses – Homeostatic plasticity and synaptic scaling

Synapses are highly complex and dynamic structures that are continuously remodelled during development, learning and memory formation. Remodelling of synaptic properties occurs also during neural damages (e.g. stroke), neurodegenerative diseases (Parkinson's or Alzheimer's disease) or drug applications (anesthetics, anticonvulsants, street drugs). On the other hand, neurons and circuits have to maintain stable interneuronal signaling over the time and under different conditions not to impair normal synaptic network functions. There are several cellular processes, which may regulate the function and transmission properties of the synapses. According to Hebbian rules for plasticity the strength of synaptic transmission can be modulated through concerted activity at individual synapses. This form of synaptic plasticity includes long-term potentiation (LTP) and long-term depression (LTD), which are thought to contribute to higher functions of the central nervous system such as learning and memory. It has been shown that LTP at one individual synapse can facilitate LTP also at neighboring excitatory synapses. Similarly, the induction of LTP at excitatory synapses elicits LTD of inhibitory synapses through Ca^{2+} -dependent activation of the phosphatase Calcineurin, leading to an increased excitability of the neuron (Lu et al., 2000). This indicates that synapses of a neuron react as a dynamic entity with limited independence one from another.

On the other hand, changes in synaptic strength can arise from homeostatic control of neuronal activity. One form of the homeostatic plasticity that attracted high interest of researchers over past few years is activity-dependent synaptic scaling. This is a mechanism by which the global synaptic strength (strength of all synapses onto a postsynaptic neuron) is adjusted or "scaled" up or down together in response to activity-dependent changes of network function (Turrigiano et al., 1998). This means that, if a neuron experiences a change in activity its equilibrium will shift in order to minimize that change. The classic experimental method of inducing homeostatic plasticity is application of pharmacological agents to block or increase synapse activity.

As shown by Turrigiano and colleagues, chronic deprivation of excitatory synaptic transmission in cortical neurons resulted in increased amplitudes of miniature excitatory postsynaptic currents (mEPSC) and increased postsynaptic glutamate sensitivity. It is believed that these changes are due to a class-switch and other alterations in AMPA-type glutamate receptors. O'Brien et al. (1998) have reported that increased mEPSC amplitude upon inhibition of the excitatory transmission in cultured spinal neurons is accompanied with accumulation of the GluR1 subunits of the AMPA receptors at synapses. In cultured neocortical cells, TTX-induced synaptic scaling proportionally increases both, GluR1 and

GluR2 accumulation at synaptic sites (Wierenga et al., 2005). A large body of evidence further indicates that synaptic activity affects postsynaptic properties apart from the glutamate receptors localization. Kirov and Harris (1999) have reported that in mature hippocampal neurons when synapses are inactivated, dendrites display a higher spine density. It was hypothesized that neurons compensate the loss of the synaptic activity potentially by increasing the number of spines. Work done by Ehlers (2003) showed that activity level controls postsynaptic composition and, moreover, that those activity-dependent changes in the PSD require ubiquitin-proteasome-mediated degradation. This promoted the idea that activity-dependent protein degradation might be a new mechanism controlling synapse remodeling, apart from gene transcription and translation, which were extensively studied in past.

Synaptic network activity may affect presynaptic function as well, but, compared to the postsynapse, there is considerable less knowledge about the activity-dependent remodeling of the presynaptic site. Using primary cultures of hippocampal neurons, as a model system, Bacci et al. (2001) have found that chronic blockade of glutamate receptors during synaptogenesis produces an enhancement of presynaptic neurotransmitter release, indicated by an increased mEPSC frequency without changes in the mEPSC amplitude or in the number of the synapses. The increase in mEPSC frequency correlates with an increase in the basal rate of SV exo-endocytotic recycling and down-regulates the interaction between Synaptophysin-Synaptobrevin/vesicle-associated membrane protein 2 (VAMP2). The lack of an effect on mEPSC amplitude is in contrast with some previously published work but this discrepancy probably occurred due to differences between culture preparations (embryonic vs. postnatal cultures) or other experimental variables (e.g. presence vs. absence of glial cells, which are known to influence both the number and the properties of newly formed synapses). Evaluating the ultra-structural changes of the synapses, Murthy et al. (2001) reported that synaptic network inactivity increases the size of all synaptic components (AZ, PSD), the total number of vesicles per synapse and the number of docked SVs, which correlates with the increased release probability. It is known that the strength of synapses might be altered presynaptically not only by changing the probability with which SV will undergo exocytosis, but also by changing the amount of the transmitter contained in each SV. This latter can be achieved by scaling the amount of vesicular transporter proteins per vesicle, which increase or decrease the vesicular loading capacity. A study done by De Gois et al. (2005) showed homeostatic scaling of vesicular glutamate (VGLUT1 and VGLUT2) and inhibitory GABA (VIAAT) transporter expression in rat neurocortical cultures. While prolonged activity deprivation increases the expression level of VGLUT1, the expression level of

GABA transporter is decreased. In contrast, prolonged hyperexcitation of neurons causes the opposite effect.

Data reported above clearly demonstrate that homeostatic synaptic compensation could occur through a variety of presynaptic and postsynaptic changes. However, for longer time ranges the question, whether the expression locus of homeostatic plasticity is pre- or postsynaptic has been discussed controversially. Wierenga et al. (2006) have tackled this issue by testing the response of cortical and hippocampal neurons to the same activity deprivation paradigm after different periods of time in vitro. Their study showed that the site of expression of homeostatic plasticity is temporally regulated. In young neurons, activity deprivation scales up excitatory synaptic strengths through postsynaptic changes in receptor accumulation, without detectable changes in presynaptic function (the amplitude but not the frequency of mEPSCs is increased). By contrast, in older neurons activity blockade produces a more complex set of changes. In addition to the postsynaptic changes, there is an additional set of presynaptic changes including increased glutamate packaging into vesicles, an increase in the number of functional release sites and an increase in vesicle release probability (now both, amplitude and frequency of mEPSCs are increased) (Fig. 7.).

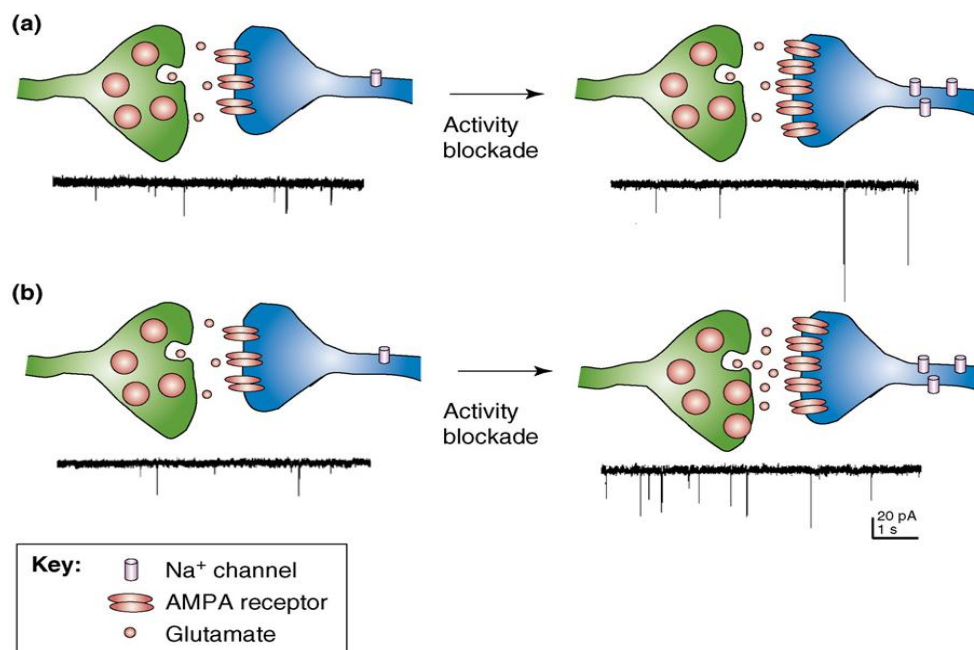


Fig. 7. Expression loci of synaptic homeostasis at central synapses (adopted from Turrigiano, 2007). (a) In young neurons (<2.5 weeks in vitro) there is purely postsynaptic response to activity blockade (receptor accumulation, increased mEPSC amplitude) (b) By contrast, older neurons (>2.5 weeks in vitro) have a mixed presynaptic and postsynaptic response (increased glutamate packaging into vesicles, number of functional release sites, SV release probability and increased both, the amplitude and frequency of mEPSCs).

Taken together in a variety of systems the existence of homeostatic plasticity phenomena is well established, but still little is known about the underlying molecular and signaling mechanisms. The activity-dependent changes in the molecular content of synapses could arise either from incorporation of new proteins or by removal of existing ones or both, but how exactly processes like gene transcription, protein synthesis and degradation are controlled by synaptic network activity is still not clear. Work performed by Ehlers brought some new insights into the understanding the activity-dependent remodeling of PSD, the role of the ubiquitination and subsequent protein degradation in homeostatic plasticity and activity-induced alternations in synaptic signaling to CREB and ERK-MAPK. However, whether the presynaptic density (CAZ) undergoes similar changes upon network activity alternations and what are molecular and signaling mechanism operating there is not known. Complete understanding of the molecular and signaling mechanisms underlying both pre- and postsynaptic homeostatic signaling will be of major importance for the understanding of processes that underlie activity-dependent refinement of neuronal circuitry, diseases and developmental disorders, during which the balance between excitation and inhibition is disrupted.

1.4. Aims of this work

There were two major aims of my PhD thesis:

I) Ultrastructural characterizations of synapses of Bsn-Pclo double mutant mice

Bassoon and Piccolo are homologous proteins that might be functionally partially redundant. Both have an exquisite presynaptic, AZ localization, and both proteins are present in synapses very early during development. Therefore, the study of mice mutant for both genes should reveal a better understanding of their role in the assembly/maturation and function of the CAZ. Double-mutant mice are not viable and the first interesting question was, whether in absence of the two proteins synapses are still formed? If yes, whether they exhibit some morphological alternations regarding to their size, number and/or density of SVs or general appearance of the pre- or/and postsynaptic compartments (length of the AZ, thickness of PSD etc).

II) Activity-dependent remodelling of presynaptic AZ

Synapses are complex and highly dynamic structures that are constantly remodelled during development, learning and memory processes. Physiologically activity-dependent changes in the synaptic properties are well described, especially for the postsynaptic compartment, however, whether similar activity-dependent changes occur on the presynaptic site remained unknown. The aim of this study was therefore to investigate whether synaptic activity may alter the molecular composition of the AZ and, if yes, what might be possible molecular mechanisms underlying this activity-dependent remodelling.

2. Materials and Methods

2.1. Materials

The chemicals used in this work were purchased from the described companies. The quality of the reagents was of analytical grade.

2.1.1. Animals

Animal lines used for organ harvesting are listed in the table 1. Animals were bred in the animal facility of the Leibniz Institute For Neurobiology, Magdeburg and in the ZENIT, Magdeburg.

Table 1. Animal lines

Animal line	Notes	Origin
C57Bl6 J cre	Wild type mice	Charles River
SV129EMSJ	Wild type mice	Jackson Laboratoeis
Bsn mutant mice	Genetic background: 50% C57Bl J cre and 50% SV129EMSJ	Altrock et al., 2003
Pclo mutant mice		A gift from T.C. Südhof Dallas, Texas, USA
Whister rats	Rattus norvegicus familiaris	Leibniz Institute for Neurobiology

2.1.2. Pharmacological reagents

Table 2. Pharmacological reagents

Compound	Biological activity	Company
D-(-)-2-Amino-5-phosphonopentanoic acid (D-AP5)	competitive NMDA antagonist	Tocris
6-Cyano-7-nitroquinoxaline-2,3-dione disodium (CNQX)	AMPA/kainate antagonist	Tocris
Picrotoxin (PTX)	GABA _A receptor antagonist	Tocris
Tetrodotoxin (TTX)	Selective inhibitor of Na ⁺ channel conductance	Tocris
Carbobenzoxy-L-leucyl-L-leucyl-L-leucinal (MG132)	potent, reversible, and cell-permeable proteasome inhibitor	Calbiochem
* Complete	Protease inhibitor cocktail tablets	Roche
* PhosStop	Phosphatase inhibitor cocktail tablets	Roche

2.1.3. Commonly used buffers

Table 3. Commonly used buffers

Cortical cultures washing buffer	10mM Tris; 300mM sucrose, pH 7.4
Cortical cultures lysis buffer	10mM Tris-HCl, pH7.4; 150mM NaCl; 2% SDS; 1% Deoxycholate, 1% TritonX-100; 1x Complete*; 1x PhosStop*
PBS	2.7mM KCl;1.5mM KH ₂ PO ₄ ;8mM Na ₂ HPO ₄ , pH 7.4
PBS-T	2.7mM KCl;1.5mM KH ₂ PO ₄ ;8mM Na ₂ HPO ₄ , pH 7.4; 0.1% Tween20

2.1.4. Cell Cultures

Cortical neuronal cultures used in this work were prepared by Sabine Opitz and Heidi Wickborn from E16-E17 rats. Primary neurons were cultured in 5% CO₂ at 37°C with humidity of 95%. All supplemented cell culture medias were sterile filtrated in sterilfirtation bottles of 0.22 µm pore size and kept until usage at 4°C.

Table 4. Cell culture media

Media and Reagents	Ingredients / Companies
DMEM (mouse culture)	2% B27(Gibco); 1mM Sodium Pyruvate 100x (Gibco); 2% AlbuMax II (Gibco); 2mM L-Glutamine 100x (Gibco); in DMEM (without: Phenolred, L-Gln, NaPyr) (Gibco)
DMEM (10% FCS)	10% FCS (Gibco); 1% Peniciline/Streptomycine 100x (Gibco); 2mM L-Glutamine 100x (Gibco) in DMEM (Gibco)
DMEM (4% FCS)	4% FCS (Gibco); 1% Peniciline/Streptomycine 100x (Gibco); 2mM L-Glutamine 100x (Gibco) in DMEM (Gibco)
NB	2% B27 (Gibco); 2mM L-Glutamine (Gibco); 1% Peniciline/Streptomycine 100x (Gibco) in Neurobasal
Distillate Water	Gibco/ Millipore
HBSS+ (with Mg ²⁺ and Ca ²⁺)	Gibco
HBSS-	Gibco
Optimem	Gibco
Ara C 1.5mM	Calbiochem
10x Trypsin	Gibco
1X Trypsin	10% 10x Trypsin (Gibco); DMEM (10% FCS)
Paraffin	Paraplast embedding medium (Fisher)

2.2. Experimental procedures

2.2.1. Genotyping of P0 animals

Newborn (P0) mice were labeled and tailcut samples were taken for DNA extraction. The tailcuts were incubated in 500 μ l of lysis buffer including freshly added Proteinase K at 55 $^{\circ}$ C for 20 min under shaking. Inactivation of the enzyme was done by incubation for 10 minutes at 98 $^{\circ}$ C and subsequently, the samples were subjected for PCR (4 μ l of the sample for one PCR reaction). The tube without tailcut sample was used as a negative control. Polymerase chain reaction (PCR) was performed using 21 μ l of master mix containing: 1pM forward primer, 1pM reverse primer, 2.5 mM MgCl₂, 0.1 units/ μ l Taq-polymerase (Qiagen), 0.2 mM dNTPs (Fermentas) in Q-solution (Qiagen, 5 X) and PCR buffer (Qiagen, 10 X). PCR products were then separated based on their size via gel electrophoresis using 1.5% of agarose in TAE buffer and voltage of 120mV. Solutions for DNA extraction, agarose gel electrophoresis, primer sequences and PCR program for genotyping of P0 animals are listed in the following tables:

Table 5. Solutions for DNA extraction, agarose gel electrophoresis

solution	composition
Lysis buffer	10mM Tris/HCl, 100mM NaCl, pH 8.0
Proteinase K-stock	10mg/ml in 40% glycerol (v/v), 10mM Tris/HCl pH7.5, 1mM calcium acetate,
6x DNA sample buffer	30% (v/v) glycerol, 50mM EDTA, 0.25% bromophenol blue, 0.25% xylene xyanol
TAE	40mM Tris, 0.2mM acetic acid, 1mM EDTA, pH 7.6

Table 6. Primer sequences for genotyping

Genotype	Forward primer	Reverse primer
Bsn WT	5'-agttgtcaagcctgttccagaagc-3'	5'-acaccgtcggaggagtagcctgt-3'
Bsn KO	5'-ggatcctgttctgaaagacttcc-3'	5'-aagcttgatcgaattggcctg-3'
Pclo WT	5'-gctctgcagaggtaaagcttgc-3'	5'-ttgtgcacgtagtcagactg-3'
Pclo KO	5'-cctgagggtcaatgtgatcagc-3'	5'-ccaagttctaattccatcagaagc-3'

Table 7. PCR program for genotyping

Proces	PCR for Bassoon		PCR for Piccolo	
	Time and temperature	Cycle	Time and temperature	Cycle
Initial denaturation	3 min at 95 $^{\circ}$ C	1		1
Denaturation	30 sec at 95 $^{\circ}$ C	35	20 sec at 95 $^{\circ}$ C	35
Annealing	40 sec at 63 $^{\circ}$ C		45 sec at 63 $^{\circ}$ C	
Extension	30 sec at 72 $^{\circ}$ C		30 sec at 72 $^{\circ}$ C	
Final extension	2 min at 72 $^{\circ}$ C	1	2 min at 72 $^{\circ}$ C	1

2.2.2. Protein concentration determination: Amidoblack protein assay

Protein concentration was determined by the colorimetric amidoblack assay. To prepare the calibration curve, 0 - 20 µg BSA and 5 - 10 µl of sample were brought to a total volume of 100 µl with dH₂O. 200 µl of amidoblack solution were added to both, the standard and sample solutions. All samples were incubated for 20 minutes at room temperature and centrifuged at maximum speed for 5 minutes. The supernatant was decanted, the pellet was washed three times with methanol-acetic acid. Finally the pellet was resuspended in 500 µl of NaOH (0.1 N). The absorption was measured at 620 nm against NaOH.

Table 8. Solutions for Amidoblack protein assay

Solution	Composition
Amidoblack solution	14.4 g amidoblack in 1 l methanol-acetic acid
Methanol-acetic acid	Methanol:acetic acid = 9:1
BSA stock solution	0.5 mg/ml

2.2.3. SDS-PAGE

In this work two different SDS-PAGE systems were used, the Laemmli and the Tris-acetate system. Proteins were separated using one-dimensional sodium dodecyl sulphate polyacrylamide gel electrophoresis (SDS-PAGE) under fully denaturing and reducing conditions (Laemmli 1970). SDS-PAGE was performed in a gradient gel: a stacking gel was layered on top of a separating gel. The samples were first incubated with SDS-sample buffer at 95°C for 5 minutes and then loaded onto the gel. Gels were allowed to run at a constant current strength of 12 mA in an electrophoresis chamber (Hoefer Mighty Small System SE 250 from Amersham Biosciences) filled with 1x electrophoresis buffer. Subsequently the gels were either stained with Coomassie blue or were used for immunoblotting. The SDS-PAGE by the Tris-acetate-system is based on the *NuPAGE-system* (Invitrogen). The system was developed for resolving big proteins and further Western blot analysis (8% to 4% gradient).

Table 9. Laemmli system

Buffer	Composition
5x SDS-sample buffer	250 mM Tris/HCl, pH 6.8, 1% (w/v) SDS, 40 % (v/v), glycerol, 4 % β -mercaptoethanol, 0.02 % bromophenol blue
Electrophoresis buffer	192 mM glycine, 0.1 % (w/v) SDS, 25 mM Tris-base, pH 8.3
4x separating buffer	0.4 % (w/v) SDS, 1.5 M Tris/HCl, pH 6.8
Separation gel (20 %)	8.25 ml separation buffer, 7.5 ml 87 % Glycerol, 16.5 ml 40 % Acrylamide, 330 μ l EDTA (0.2 M), 22 μ l TEMED, 120 μ l 0.5 % Bromophenol blue and 75 μ l 10 % APS
Separation gel (5 %)	8.25 ml separation buffer, 17.94 ml dH ₂ O, 1.89 ml 87% Glycerol, 4.12 ml 40% Acrylamide, 330 μ l EDTA (0.2 M), 22 μ l TEMED and 118 μ l APS.
Stacking gel (5 %)	6 ml stacking buffer, 7.95 ml dH ₂ O, 5.52 ml 87 % Glycerol, 3.90 ml 30 % Acrylamide, 240 μ l EDTA (0.2 M), 240 μ l 10 % SDS, 17.2 μ l TEMED, 30 μ l Phenol red and 137 μ l 10 % APS

Table 10. SDS-PAGE under reducing conditions by the Tris-acetate system

Buffer	Composition
4x stacking and separation gel	0.5 M Tris-acetat; pH 7.0
Rotiphorese 30	30 % Acrylamid, 0.8 % Bisacrylamide (Carl Roth)
Separation gel (8 %) (for 5 gels)	3.2 ml 4x buffer, 3.47 ml Rotiphorese 30, 3 ml 87 % Glycerine, 3.28 ml H ₂ O, 10 μ l TEMED, 50 μ l Ammoniapersulfate, 10 μ l Bromophenolblue
Separation solution (3.5 %) (for 5 gels)	3.25 ml 4x buffer, 1.52 ml Rotiphorese 30, 3 ml 87 % Glycerine, 7.48 ml H ₂ O, 10 μ l TEMED, 50 μ l Ammoniumpersulfate
Stacking-gel	2.5 ml 4x buffer, 1 ml Rotiphorese 30, 2.3 ml 87 % Glycerine, 4.2 ml H ₂ O, 10 μ l TEMED, 60 μ l 10 % Ammoniumpersulfate, 5 μ l Bromophenol blue
5x SDS loading buffer	500 mM Tris-HCl, 20 % Glycerine, 4 % SDS, 1 mM EDTA, 0.001 % Bromophenol blue, pH 8.5. 30 mg/ml of DTT (200 mM) was added prior to use.
20x gel running buffer	1 M TrisBase, 1 M Tricine, 2 % SDS

2.2.4. Coomassie staining of SDS-polyacrylamide gels

Polyacrylamide gels were stained with Coomassie solution for 30 minutes. Proteins were visualized by incubating the gel in destaining solution for 2 hours or overnight by shaking. Gels were visualized by Odyssey Infrared Imaging System (LI-COR Bioscience) or alternatively, the destained gels were incubated for 15 minutes with drying solution for preservation and mounted between two cellophane membranes in a drying device.

Table 11. Solutions for Coomassie staining

Coomassie blue staining solution	1 mg/l Coomassie brilliant blue R-250, 60 % (v/v) methanol, 10 % (v/v) acetic acid
Destaining solution	7 % (v/v) acetic acid, 5 % (v/v) methanol
Drying solution	5 % (v/v) glycerin, 50 % (v/v) methanol

2.2.5. Western blotting

Proteins were electrotransferred from polyacrylamide gels to Millipore Immobilon-FL transfer membranes (polyvinylidene fluoride membrane (PVDF)). The transfer was performed in blotting buffer at 4°C for 1.30h with 200 mA for Tris-Glycine gels, or 3.30h with 250mA for Tris-Acetate gels.

Table 12. Blotting buffers

Buffer	Composition
Blotting buffer for Tris-acetate	25 mM Bicine, 25 mM BisTris, 1 mM EDTA, 5% methanol
Blotting buffer for TrisGlycin	192 mM Glycine, 0.2 % (w/v) SDS, 18 % (v/v) methanol, 25 mM Tris-Base, pH 8.3

2.2.6. Immunoblot detection

After transfer PVDF membranes were briefly pre-wet in 100% methanol, rinse with distilled water and dry at room temperature. Then membranes were wetted in PBS for several minutes. Blots were incubated at 4°C overnight with the primary antibody diluted in PBS-T containing 5 % of BSA and 0.025% of sodium azide. After three washing steps with PBS-T for 10 minutes each time, the membranes were submerged in peroxidise-coupled secondary antibodies (diluted in 1% of BSA) for 1 hour at room temperature. Membranes were rinsed again three times with PBS-T and immunodetection was carried

out employing ECL films (GE Healthcare, Amersham Hyperfilm™ ECL), which were developed automatically using Agfa Curix 60 developing machine.

For all quantitative immunoblotting, protein transfer and incubation with primary antibodies were done in the same manner as described above. Fluorescently-labeled secondary antibodies were diluted in PBS-T containing 5 % of BSA and 0.01% of SDS (addition of SDS reduce membrane background, particularly when using PVDF), and membranes were incubated for 1 hour at room temperature. After four washing steps in PBS-T and two in PBS, membranes were scanned in the appropriate channels (700 or 800 nm) using Odyssey Infrared Imagine System. From obtained intensity for each band the background subtraction was made (background intensity was taken as mean of the three empty places from the membrane).

2.2.7. Immunocytochemistry

The cells were fixed with 4% paraformaldehyde, 4% sucrose in PBS, pH 7.4, for 10 minutes at room temperature. Prior to immunostaining, the cells were block for 1 hour in PBS containing 10% fetal calf serum (FCS), 0.1% glycine and 0.3% TritonX-100. Primary antibodies were applied overnight at 4°C. After three washing steps with PBS at room temperature, the Cy3- 488- or Cy5-labelled secondary antibodies were applied to the cells for one hour (at room temperature). Both, primary and secondary antibodies were diluted in PBS containing 3% FCS. Coverslips were maintained on slides with Mowiol (Calbiochem) including and were incubated overnight at 4°C before microscopy analysis.

Images were taken with Zeiss Axioplan2 (Zeiss Microimaging), Spot RT-KE camera (Diagnostics Instruments, Inc.) and MataVue software (Molecular Devices). For each couple of coverslips (treated vs. control) the same exposure time was taken.

Primary and secondary antibodies used for immunoblotting and immunocytochemistry are listed in Tables 13 and 14:

Table 13. Primary antibodies for Western blot and Immunostaining

Antibodies	Species	WB dilution	ICC dilution	Company
AKAP 150 (N-19: sc-6446)	goat	1:500		Santa Cruz
Bassoon (Sap7f)	rabbit	1:2.000	1:2.000	Tom Dieck et al., 1998
ERC 1b/2 (ELKS 1b/2)	rabbit	1:1.000		Synaptic Systems
Homer 1 (VesL1)	rabbit	1:1.000	1:2.000	Synaptic Systems
Liprin alpha3	rabbit	1:1.000		Synaptic Systems
MAP2 (clone HM-2)	mouse		1:2000	Sigma Aldrich
Munc13-1	rabbit	1:1.000	1:1.000	Synaptic Systems
Piccolo	guinea pig	1:1.000	1: 500	Dick et al., 2001
PSD-95 (clone K28/43)	mouse	1:2000		Upstate
RIM1,2 (Zn-finger domain)	rabbit	1:1.000	1:1.000	Synaptic Systems
SV2B	rabbit	1:1.000	1:1.000	Synaptic Systems
Synapsin	rabbit	1:1.000		Synaptic Systems
Synaptophysin	rabbit		1:5.000	Gift of Dr. R. Jahn
Synaptophysin (clone SVP-38)	mouse	1:1000		Sigma Aldrich
Synaptophysin 1	guinea pig		1:2.000	Synaptic Systems
Syntaxin 1	mouse	1:1000		Synaptic Systems
Syntaxin 6	rabbit	1:1.000		Synaptic Systems
Tubulin-beta III	mouse	1:5000		Sigma Aldrich
VGLUT1	rabbit		1:1000	Synaptic Systems
Voltage-gated-Ca ²⁺ channel (P/Q-type, alpha-1A subunit)	rabbit		1:1000	Synaptic Systems

Table 14. Secondary antibodies for Western blot and Immunostaining

Antibodies	Species	WB dilution	ICC dilution	Company
anti-mouse, rabbit or guinea pig IgG, Alexa Fluor™ 488 - conjugated	goat or donkey		1:2.000	Invitrogen
anti-mouse, rabbit or guinea pig IgG Cy3™-conjugated	goat or donkey		1:2.000	Jackson Immuno Research
anti-mouse, rabbit or guinea pig IgG Cy5™-conjugated	goat or donkey		1:1.000	Jackson Immuno Research
anti-mouse, -rabbit or guinea pig IgG, peroxidase-conjugated	goat, donkey or rabbit	1:20.000		Jackson Immuno Research
anti-mouse, -rabbit or goat IgG Alexa 680	goat or donkey	1:20.000		Invitrogen
anti-mouse or -rabbit IgG, IRDye™-800CW	Goat or donkey	1:20.000		Rockland

2.2.8. Electron microscopy (EM)

Mouse hippocampal cultures were prepared by Dr. Anna Fejtova from P0 mice following the protocol described by Goslin et al. (1998).

Neurons were grown on coverslips for 16 days and subsequently processed for conventional EM. After removing the media, cells were fixed with buffer containing 1% formaldehyde and 1% glutaraldehyde in 0.1M NaPi (pH 7.4) for 10 minutes at room temperature. After three washing steps in 0.1M NaPi and three washing steps in 0.1M cacodylate buffer cells were incubated for 1hour in 1% OsO₄. Then, dehydration in a series of several ethanol concentrations (50%, 70%, 80%, 90%, 96% up to 100%) was performed with a blocking staining with 2% uranyl acetate during the 70% ethanol step for 1 hour. The coverslips were then embedded in Durcupan by sandwiching between two sheets of plastic foil for next 48h. After that the pieces of selected cells were cut out and glued on Durcupan blocks over night. The ultrathin sections (50nm) were obtained with an Ultracut E (Reichert-Jung, Heidelberg, F.R.G.) and mounted on grids. Samples were examined and photographed at 12500x magnification using Leica EM 912 Omega electron microscope.

2.3. Data analysis

In general, images were adjusted and analyzed using ImageJ (NIH, Bethesda, MD), Metamorph, Photoshop (Adobe) or OpenView software (written by N. Ziv; Tsuriel et al., 2006). Images for EM study were processed by ImageJ. Synaptic parameters were measured as described in Results section (page 31). Quantitative Western blot analyses were done using Odyssey Infrared Imaging System (LI-COR). All statistical analyzes were performed with Prism 4 software (GraphPad Software) using one-way ANOVA or t-test (as indicated in each experiment).

3. RESULTS

3.1. Ultrastructural characterization of Bassoon-Piccolo double mutant mice

Mice heterozygous for the Bassoon mutations (*Bsn*^{+/-}) were crossed with heterozygous Piccolo-mutant mice (*Pclo*^{+/-}) to produce animals homozygous for both genes (Bsn-Pclo double mutants). Genotyping of newborn (day P0) animals was performed by PCR (primers and conditions are given in Material and Methods) (Fig. 8. A). In contrast to *Bsn* and *Pclo* single mutant mice, which are viable at the birth, double mutants die a few hours after birth probably because of reduced breathing rate and/or dehydration, as they do not feed (Fig. 8. B).

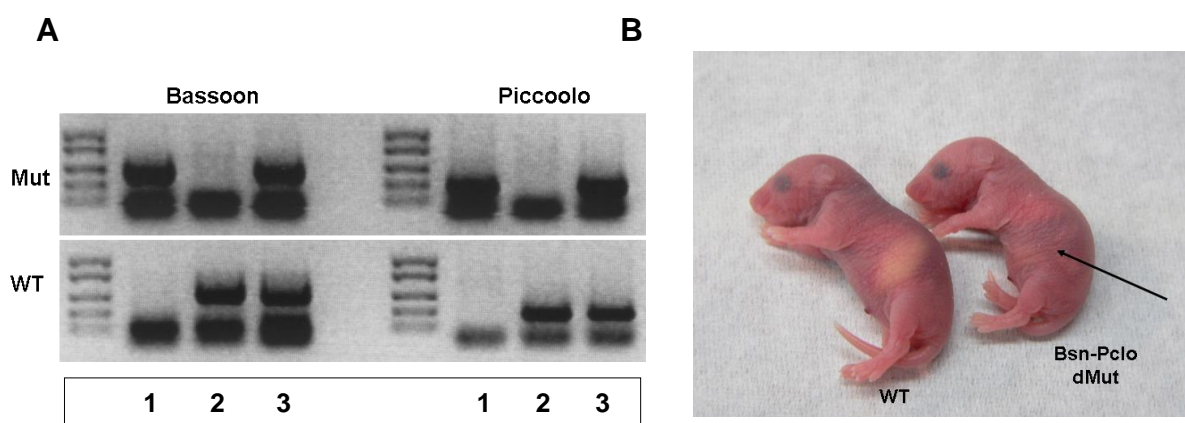


Fig. 8. Basson-Piccolo double mutant mice. A. Genotyping of three (1,2,3) P0 animals by PCR. Note that animal 1 is Bassoon-Piccolo double mutant, animal 2 is WT and animal 3 is heretozygous for both genes. B. Bassoon-Piccolo double mutant mice are born but die a few hours after birth. The lack of milk in their stomach (arrow) suggests that they are not able to feed and therefore may die because of dehydration.

To evaluate synapse formation and synaptic structure a cell culture system had to be established. Banker-type primary cultures of newborn homozygous mutants and wild-type littermates were established for this purpose by Dr. Fejtova in our laboratory. In double-mutant background synapses can be formed as shown by immunostaining of hippocampal cultures using anti-Synapsin antibody as synaptic marker (Fig. 9. A). Similarly postsynaptic marker proteins can be detected as well (Fejtova personal communication). By contrast, staining with Bassoon and Piccolo antibodies completely abolished the fluorescence signal in double-mutant cultures (Fig. 9. B and C). There were no obvious differences between cultured neurons from WT and *Bsn-Pclo*-dMut cultures regarding to cells shape, culture density or survival. Moreover, as tested in autaptic culture systems of hippocampal neurons, synapses in double mutant background are

functional and display a phenotype similar to Bsn mutants (A. Meyer, A. Siegler & C. Rosenmund, personal communication; Altmann et al., 2003).

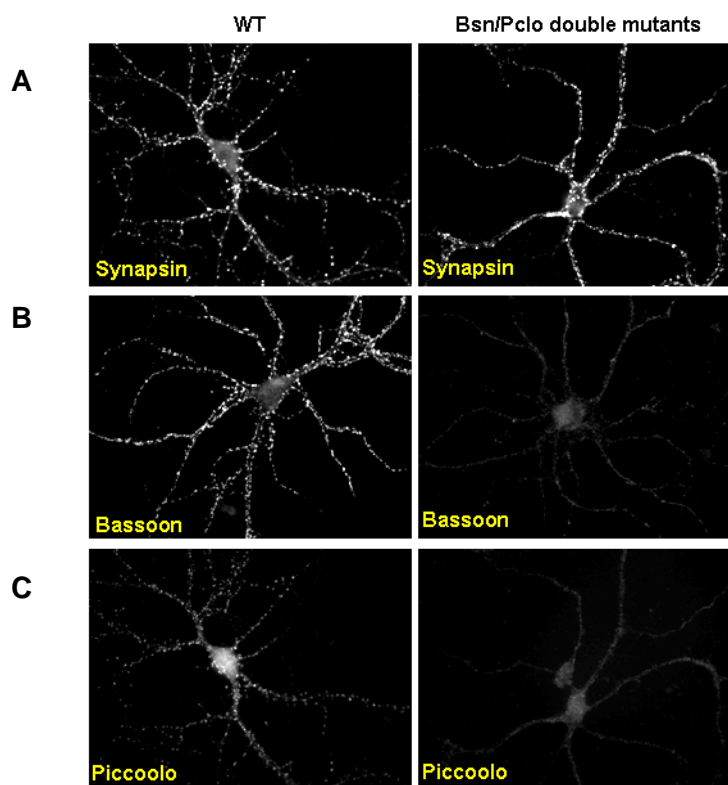


Fig. 9. Staining of the cultured hippocampal neurons from WT and Bsn-PcLo double mutant mice for synaptic proteins. Cultured hippocampal neurons (16 DIV) from WT or Bsn-PcLo double mutant mice were fixed, permeabilized and stained for synaptic marker protein (Synapsin, A) or CAZ proteins Bassoon (B) and Piccolo (C). The figure was provided by Dr. Fejtova.

In order to evaluate the consequences of Bsn and PcLo deficiencies for synaptic structure and function we carried out a morphological analysis of central synapses from Bsn-PcLo double mutant mice using electron microscope (EM). Primary hippocampal neurons from double-mutant and comparable wild-type animals were grown for 16 days in culture and processed for conventional EM including formaldehyde and glutaraldehyde fixation and Durkopan embedding. For this study 50nm ultra-thin sections were mounted on grids and further post contrasted utilizing uranyl acetate. In total 258 synapses from 4 WT and 325 synapses from 4 double mutant animals were analysed. In each synapse the following parameters were measured (Fig. 10.): (a) AZ length characterized as the length of PSD; (b) Number of SVs in the proximal zone (inside the semicircle around the AZ); (c) Number of docked vesicles per 100 nm of AZ (docked vesicles defined as SVs, which are lying within 50nm distance from the presynaptic plasma membrane, divided by length of the active zone multiplied by 100); (d) Width of the postsynaptic density (PSD) measured in the centre of the synaptic junction and (e) Number of potential PTVs in presynaptic buttons (as potential PTVs are counted only 80 nm dense core vesicles).

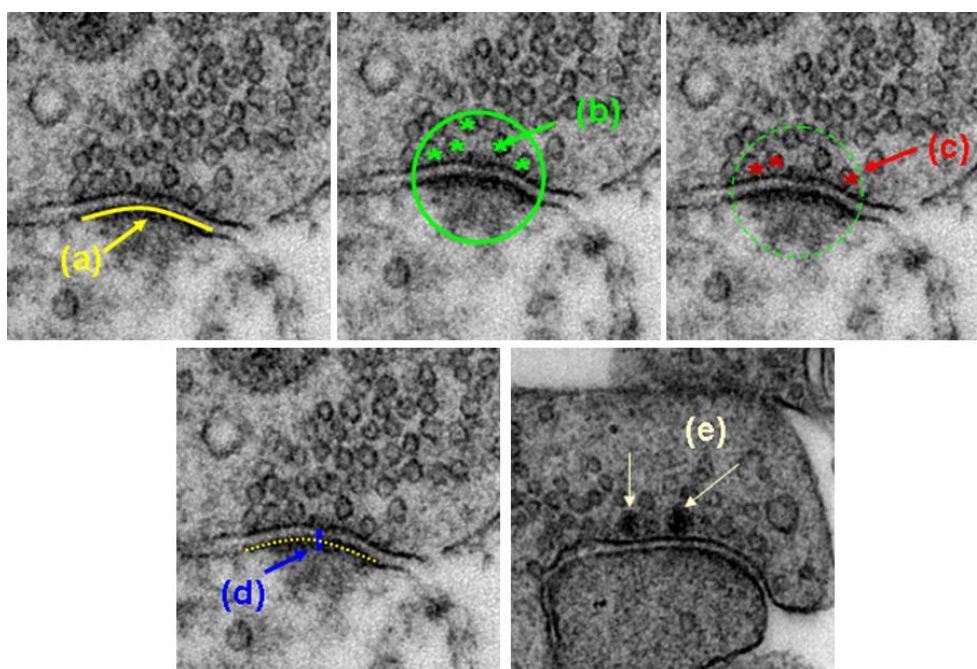


Fig. 10. Parameters that morphologically define the synapses

This evaluation revealed that in Bsn-Pclo double mutants the thickness of the PSD was significantly reduced compared to WT animals ($0.026 \pm 0.001 \mu\text{m}$ for WT vs. $0.016 \pm 0.0008 \mu\text{m}$ for Bsn-Pclo double mutants; mean \pm SEM; $P=0.0017$). Also, the number of 80nm dense core vesicles in presynaptic buttons was significantly reduced in double mutant mice as compared to WT (0.5 ± 0.07 WT vs. 0.13 ± 0.04 Bsn-Pclo double mutants; mean \pm SEM; $P=0.0049$). We assume that these 80nm dense core vesicles represent AZ transport vesicles (PTVs) but in the absence of two major constituents, Bsn and Pclo, one can name them as “potential PTVs”.

No significant differences were found in the AZ-length ($0.36 \pm 0.01 \mu\text{m}$ WT vs. $0.38 \pm 0.01 \mu\text{m}$ Bsn-Pclo double mutants; mean \pm SEM; $P=0.5043$) and in the number of SVs in the proximal zone (4.75 ± 0.14 WT vs. 4.35 ± 0.63 mutants; mean \pm SEM; $P=0.5550$). The number of docked SVs per AZ was not significantly different, although there was clear tendency in the whole data set towards less docked vesicles in double mutants (0.45 ± 0.01 WT vs. 0.38 ± 0.03 double mutants; mean \pm SEM; $P=0.1388$). The number of docked vesicles was significantly reduced in 3 out of 4 double mutant animals analyzed (Table 15, Fig. 11.).

Table 15. Morphometric analysis of synapses in cultured hippocampal neurons of WT and Bassoon-Piccolo double mutant mice

parameters	control		Bsn-Pclo double mutants	
	N (animals/ synapses)	mean \pm SEM	N (animals / synapses)	mean \pm SEM
AZ-length (μ m)	4 /	0.36 \pm 0.01	4	0.38 \pm 0.01
dSV/100nm AZ	4 /	0.45 \pm 0.01	4	0.38 \pm 0.03
SVs in PZ	4	4.75 \pm 0.14	4	4.35 \pm 0.63
PSD- thickness(μ m)	4	0.026 \pm 0.0008	4	0.016 \pm 0.002**
Number of "PTVs"	4	0.57 \pm 0.07	4	0.13 \pm 0.04**
	Total 136 "PTVs" in 258 synapses		Total 47 "PTVs" in 325 synapses	

Data were obtained from high-magnification electron micrographs of synapses from 4 WT and 4 Bsn-Pclo double mutant animals (n-number of animals). The total number of analysed synapses (N) is 258 of WT and 325 of Bsn-Pclo double mutants. dSV-docked synaptic vesicles; SEM-standard error of the mean; **p< 0.01 All analyses were carried out by investigator without any knowledge of the genotype. Statistical analysis (t-test) was performed using GraphPad Prism 4 program.

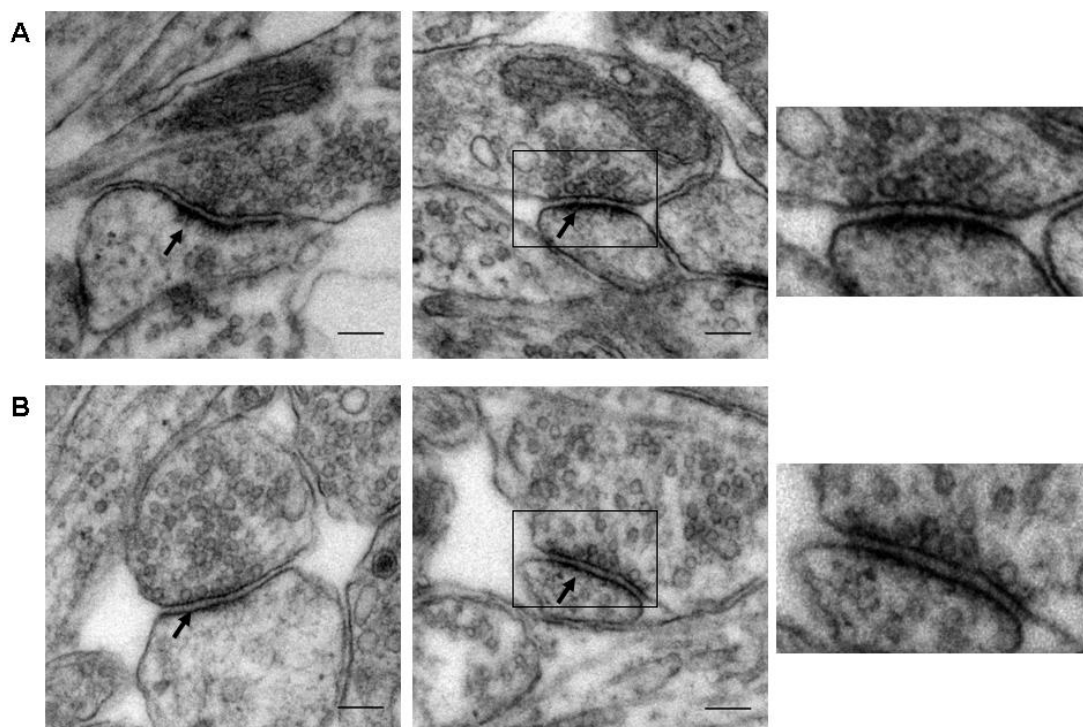


Fig. 11. The ultra-structure of synapses from hippocampal neurons in culture (16 div). The difference in the width of PSD (arrows) in WT (A) and Bsn-Pclo double mutants (B) is apparent from individual examples. Samples were examined and photographed at 12500x magnification using Leica EM 912 Omega electron microscope. Scale bar 100nm. Right panels provide higher magnifications of selected area.

Taken together, the ultrastructural examination of Bsn-Pclo double mutant synapses revealed unexpected change in the postsynaptic compartment. On the other hand the reduced number of 80-nm dense-core precursor vesicles is in line with the assumption that Bsn and Pclo are necessary for PTVs formation. The fact that some of those vesicles are still present in double-mutant mice suggests that other molecules are also carried by PTVs. These can be e.g. RIMs and/or Munc13s, Ion channels, neurotrophic and growth factors, adhesion molecules or other signalling molecules. Based on the results we can hypothesize that Bsn and Pclo are not necessary for synapse formation, but they might be crucial for their maturation during later development.

3.2. Activity-dependent remodelling of presynaptic active zone

3.2.1. Activity-dependent modulation of synaptic proteins expression level

Physiologically, a variety of activity-dependent changes in the synaptic properties have been described. While postsynaptic molecular mechanisms have been analyzed to some extent, our knowledge about the molecular mechanisms underlying the activity-dependent remodelling of the presynaptic side is sparse.

To examine whether synaptic activity may alter the molecular composition of the active zone, cultured cortical neurons were used as a convenient model system for various activity-related pharmacological manipulations. Global synaptic network activity was altered pharmacologically by application of glutamate antagonists (APV and CNQX) which leads to silencing of synaptic transmission, or GABA_A receptor blocker (PTX) which increases global activity by network disinhibition. To examine the effect of the treatment on expression level of selected proteins, lysates from treated and control cells were subjected to quantitative Western blot analysis using the Odyssey system. Cortical neurons were initially maintained in culture in the absence of receptor antagonists for 21 days, and subsequently, incubated for 48 hrs, either in media containing APV and CNQX (inhibited cells), or in media containing PTX (active cells). Control neurons were kept in control media (Fig. 12.).



Fig. 12. Experimental setup. Cortical neurons were initially maintained in culture in the absence of receptor antagonists for 21 days (yellow) and subsequently, incubated for 48 hrs, either in media containing APV and CNQX (blue), or in media containing PTX (red).

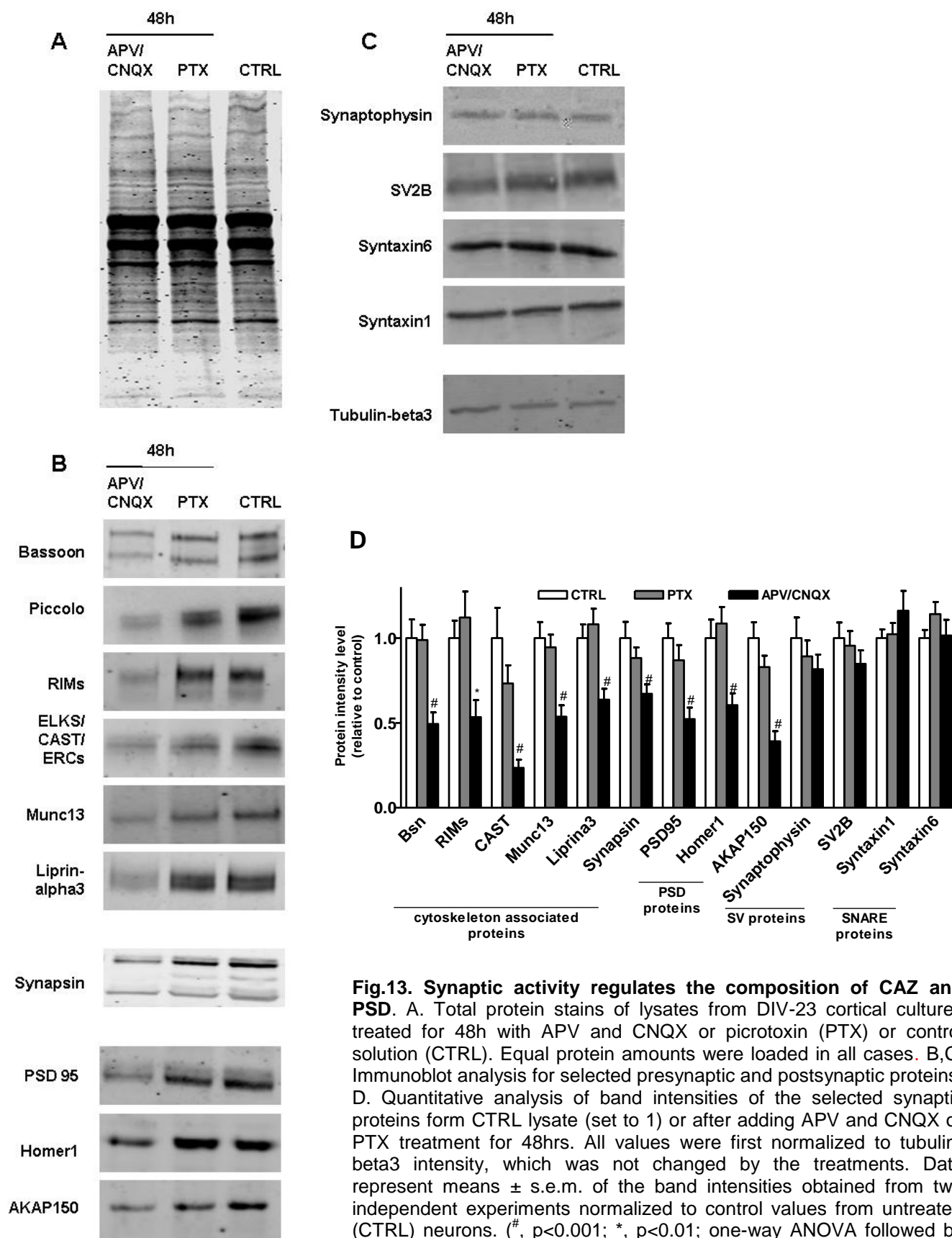
Cells were lysed under very harsh conditions, i.e., in a buffer containing 1% TritonX-100, 1% deoxycholate and 2% SDS, detergents which help to extract and solubilize majority of the cellular proteins. Total protein levels were determined by an amido black assay and equal amounts of the lysates (7-10 μ g per lane) was loaded onto a gel (fig. 13. A.). All data presented in Fig. 13. were obtained from two independent experiments. In each experiment three samples per condition were loaded onto the gel in triplicates. Protein band intensities were normalized to the intensity of tubulin-beta3 staining, expression level of which was not influenced by activity manipulations (Fig. 13. C).

The results showed that, in three weeks old cultures, prolonged inhibition of excitatory synaptic transmission (48h treatment with 50 μ M APV and 10 μ M CNQX) significantly decreases the expression level of the presynaptic, CAZ proteins including Bassoon, Piccolo, RIMs, Munc13, CAST/ELKS/ERCs and Liprin-alpha and the presynaptic scaffolding protein Synapsin as well as some of the postsynaptic scaffold proteins (PSD-95, AKAP-150, Homer), as compared to the synaptic network excitation (48h of 50 μ M PTX application) or the control state (Fig. 13. B). On the other hand, the same condition does not influence the expression of synaptic vesicle proteins, such as SV2B and Synaptophysin, or the SNARE-family proteins (Syntaxin1 and Syntaxin6) (Fig 13. C). The quantitative analysis also revealed that in our culture system further excitation of synaptic network (48hrs of PTX treatment) did not alter the protein composition as compared to the control state probably due to already high level of its basal activity (Table 16, Fig. 13.).

Table 16. Percent change (relative to control) in synaptic protein levels 48hrs after adding PTX or APV/CNQX

Protein	PTX_48hrs Protein levels: % of control	APV/CNQX_48hrs Protein levels: % of control
Bassoon	98.85 \pm 8.9	49.39 \pm 6.7 ^{***}
RIMs	112.15 \pm 15.2	53.40 \pm 10.0 ^{**}
CAST/ELKS/ERCs	73.30 \pm 10.6	23.50 \pm 4.9 ^{***}
Munc13	94.50 \pm 7.4	53.65 \pm 6.7 ^{***}
Liprin_alpha3	108.05 \pm 9.1	63.70 \pm 6.3 ^{***}
Synapsin	88.20 \pm 6.2	67.15 \pm 5.5 ^{***}
PSD95	86.95 \pm 8.9	52.25 \pm 6.8 ^{***}
Homer1	108.55 \pm 9.7	60.45 \pm 6.9 ^{***}
AKAP150	82.90 \pm 6.7	39.20 \pm 5.9 ^{***}
Synaptophysin	89.20 \pm 9.3	81.65 \pm 8.5
SV2B	95.50 \pm 8.5	84.85 \pm 7.8
Syntaxin1	102.30 \pm 6.6	116.15 \pm 11.0
Syntaxin6	114.15 \pm 7.0	101.55 \pm 9.1

Note all over reduction in the intensity level for all CAZ-proteins (Bassoon, RIMs, CAST/ELKS/ERCs, Munc13, Liprin; Synapsin and selected postsynaptic scaffolds (PSD95, Homer1, AKAP150) after activity deprivation. No statistically significant changes in the expression of SV (SV2B, Synaptophysin) and SNARE proteins (Syntaxin1 and 6) (***, $p < 0.001$; **, $p < 0.01$, one-way ANOVA followed by Bonferoni post test. Data represents mean \pm SEM)



3.2.2. Activity-dependent reduction of CAZ proteins at synaptic sites

The decrease in expression level of CAZ-associated proteins during synaptic scaling induced by silencing of network activity could be due to downscaling of proteins level at all synapses or to an all-over reduction of synapse number. To distinguish between these two possibilities comparative immunocytochemical experiments were performed. DIV-21 neurons grown under control conditions or treated for 48hrs with APV and CNQX were fixed, permeabilized with 0.3% of TritonX-100 and stained with antibodies against various synaptic proteins. Co-staining with an anti-MAP2 antibody was used to select 20 μ m long dendritic segments 10 μ m apart of the cell body. First, the number of puncta positive for staining with anti-Synaptophysin antibody in such dendritic segments was analyzed. No differences were found between control and treated cells (41.51 ± 1.69 vs. 43.28 ± 1.754 puncta per 20 μ m dendrite; mean \pm SEM, n=59 vs. 54 cells) showing that upon activity deprivation there is no change in overall number of synapses (Fig.14.).

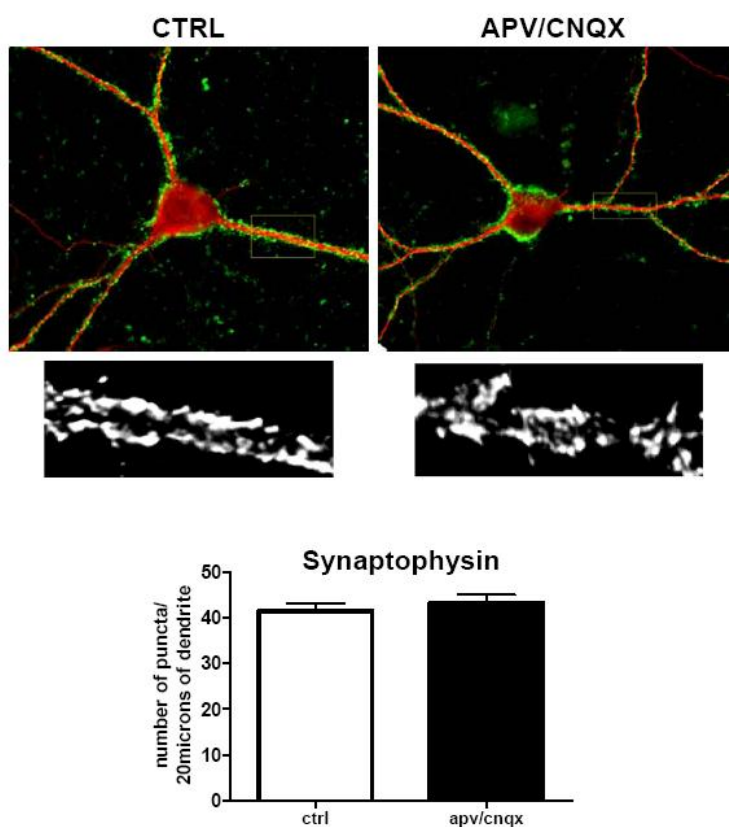


Fig.14. Overall number of synapses revealed by Synaptophysin staining was unchanged upon synaptic network activity deprivation. Cortical neurons (after 21 DIV) were treated for 48hrs with 50 μ M APV and 10 μ M CNQX or kept in control solution (CTRL). The graph represents the number of Synaptophysin positive puncta (stained in green) counted along MAP2 staining (red) per 20 μ m of the dendrite. Data were obtained from two independent experiments; in total 59 control and 54 treated cells were analyzed (the number of Synaptophysin positive puncta per 20 μ m is displayed: 41.51 ± 1.69 (CTRL) vs. 43.28 ± 1.754 (APV/CNQX); mean \pm SEM, t-test).

Also, no quantitative changes were observed in immunostainings for synaptic vesicle proteins SV2B (37.92 ± 2.656 vs. 37.69 ± 1.970 puncta per 20 μ m of the dendrite, mean \pm SEM, n=12 vs. 16 cells) and Synaptotagmin (23.13 ± 2.503 vs. 21.22 ± 2.454 puncta per 20 μ m of the dendrite, mean \pm SEM, n=9 vs. 8 cells) (Fig. 15).

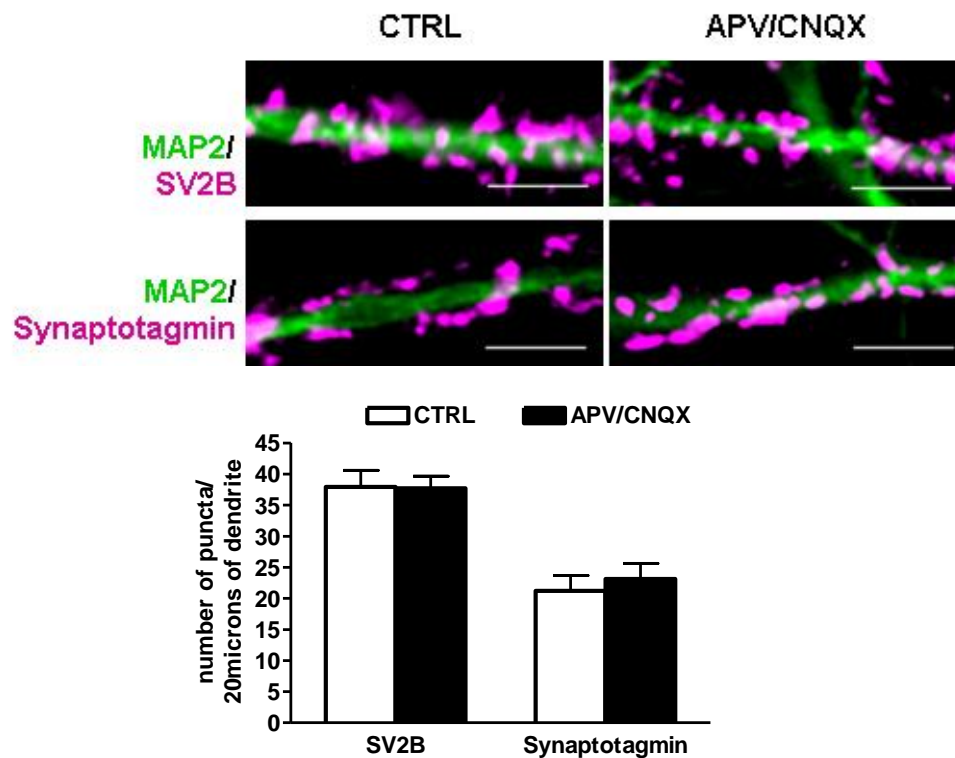


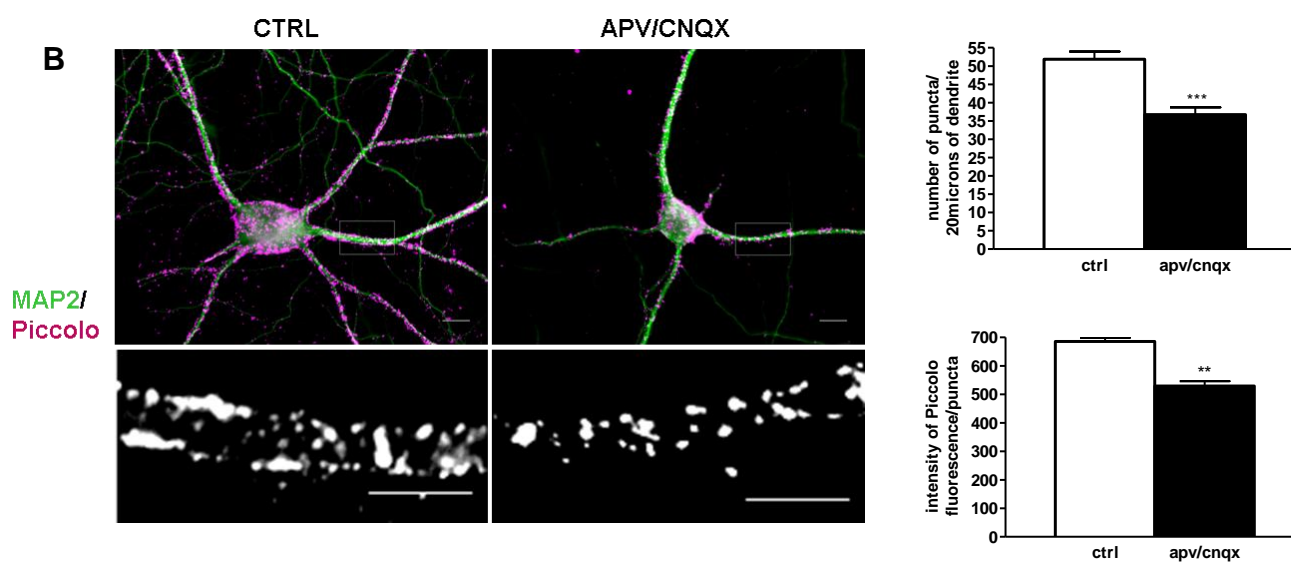
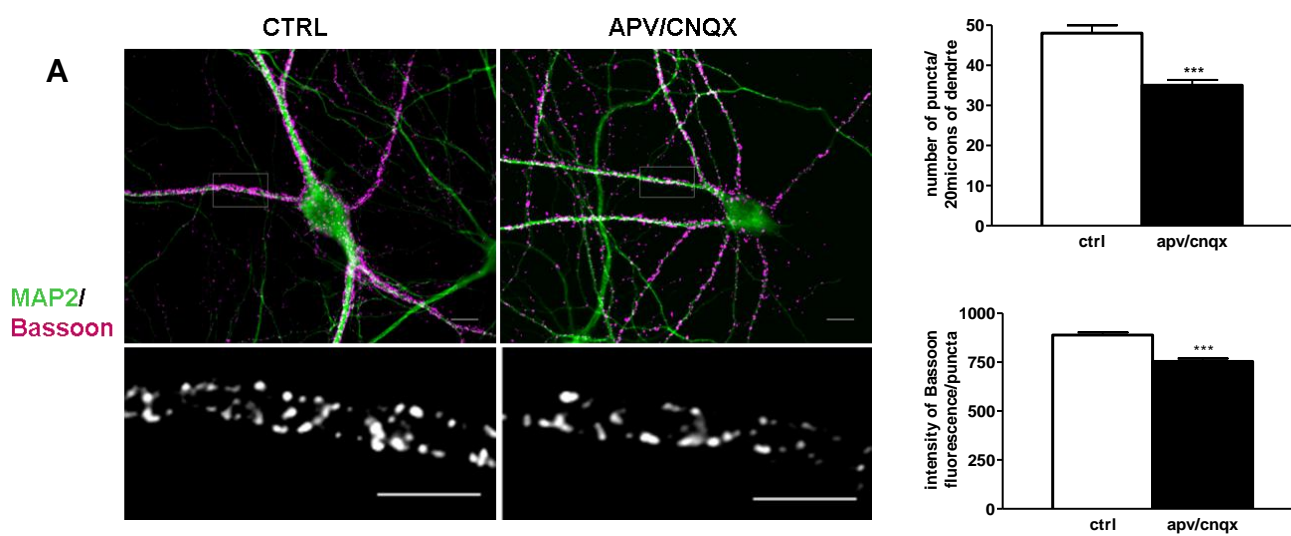
Fig.15. Prolonged synaptic network inhibition did not alter the amount of SV proteins (SV2B, Synaptotagmin). Cultured cortical neurons (21 DIV) were either treated with APV/CNQX for 48hrs or kept in control solution before fixation, permeabilization and staining for selected proteins. Scale bar, 5 microns. Quantitative analysis showed no statistically significant changes in the number of protein puncta per 20 microns of dendrite. SV2B (37.92 ± 2.656 vs. 37.69 ± 1.970 puncta per $20 \mu\text{m}$ of the dendrite, mean \pm SEM, $n=12$ vs. 16 cells) and Synaptotagmin (23.13 ± 2.503 vs. 21.22 ± 2.454 puncta per $20 \mu\text{m}$ of the dendrite, mean \pm SEM, $n=9$ vs. 8 cells). The observed difference between SV2B and Synaptotagmin positive number of puncta might be due to different sensitivities of anti-SV2B and anti-Synaptotagmin antibodies that have been used in the experiment.

Analogous quantitative analysis using antibodies against CAZ proteins Bsn, Pclo, Munc13 and RIMs (Fig. 16.) and postsynaptic scaffolding protein Homer1 (Fig. 17.) revealed a dramatic decrease in the number of immunoreactive puncta in silenced neurons. Furthermore, the fluorescence intensity of all CAZ-proteins was also changed upon activity blockade (Table 17.).

Table 17. APV/CNQX treatment reduces the levels of CAZ and PSD proteins in synapses

Protein	Number of puncta/ 20 microns of dendrite				Fluorescence intensity/ 20 microns of dendrite			
	N	CTRL	n	APV/CNQX_48hrs	N	CTRL	N	APV/CNQX_48hrs
Bassoon	39	48.03 ± 1.96	38	35.03 ± 1.33***	1787	888.9 ± 13.07	1444	753.7 ± 14.67***
Piccolo	38	51.84 ± 2.12	36	36.72 ± 1.97***	1021	685.6 ± 13.37	631	529.5 ± 16.86***
RIMs	33	45.58 ± 1.25	36	30.61 ± 1.01***	1504	691.1 ± 14.73***	1102	1119 ± 24.11
Munc13	25	56.28 ± 5.07	28	42.01 ± 3.53**	527	471.7 ± 7.76	440	333.5 ± 6.44***
Homer1	15	53.6 ± 3.36	14	40.57 ± 3.19**				

The number of protein puncta and relative synaptic fluorescence intensity per 20 microns of dendrite from control (CTRL) and APV/CNQX treated cells (21 DIV). Data represent means ± SEM. n-number of cells per each condition; N- number of puncta whose intensity was measured. ***P<0.001; **P<0.01, t-test



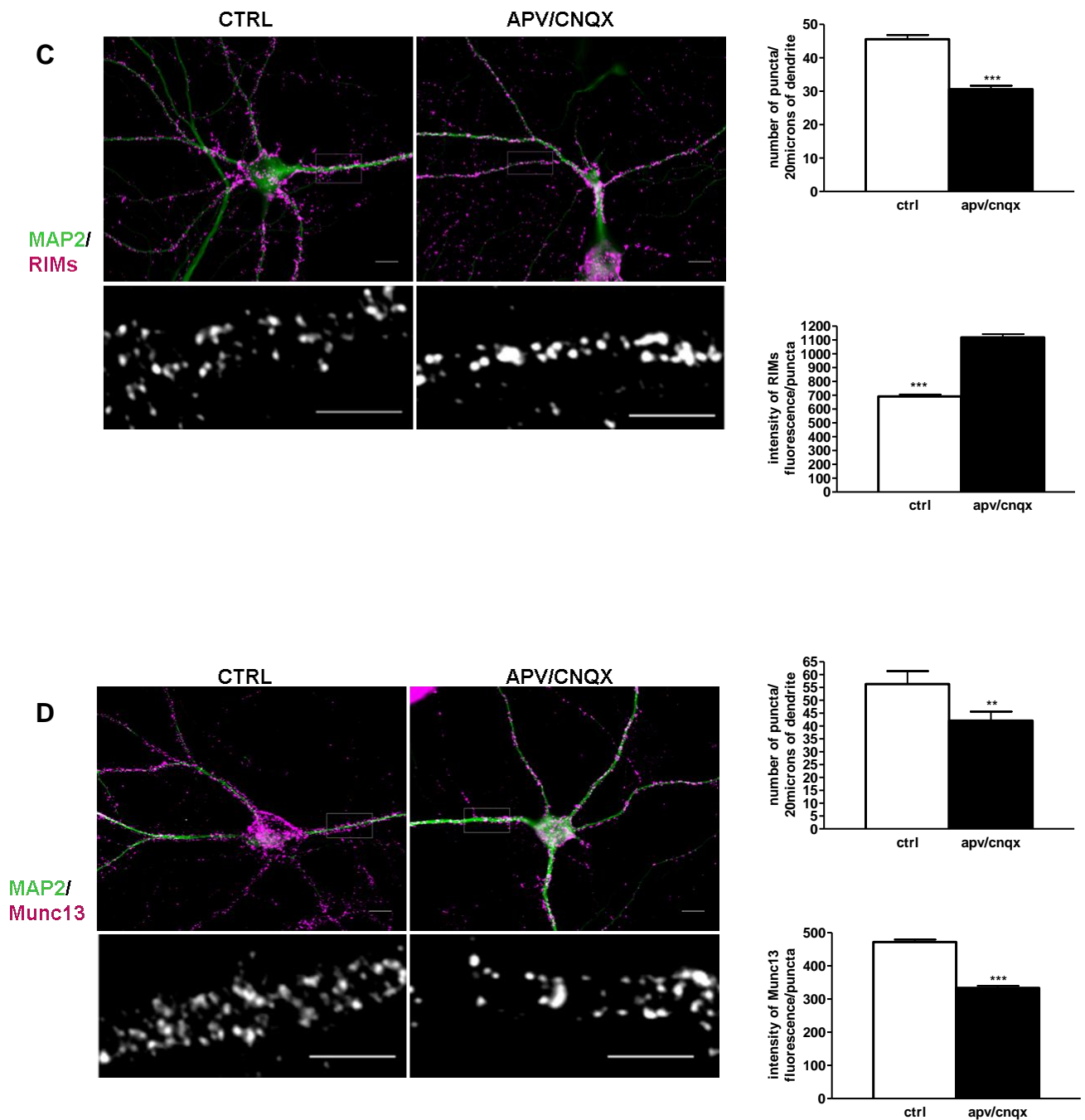


Fig. 16. Activity-dependent reduction of CAZ proteins at synaptic sites. Cultured cortical neurons (21 DIV) were treated with either APV/CNQX for 48hrs or kept in control solution (CTRL). Cells were fixed, permeabilized and stained for CAZ-specific proteins: (A) Bassoon, (B) Piccolo, (C) RIMs and (D) Munc13. Quantitative analysis showed changes in both, number of CAZ protein puncta per 20 microns of dendrite and in synaptic fluorescence intensity. Scale bar, 10 microns in overlay picture, 5microns in selected region of interest. Data represent means \pm s.e.m. ** $P < 0.01$; *** $P < 0.001$ relative to control (Table 17.), t-test.

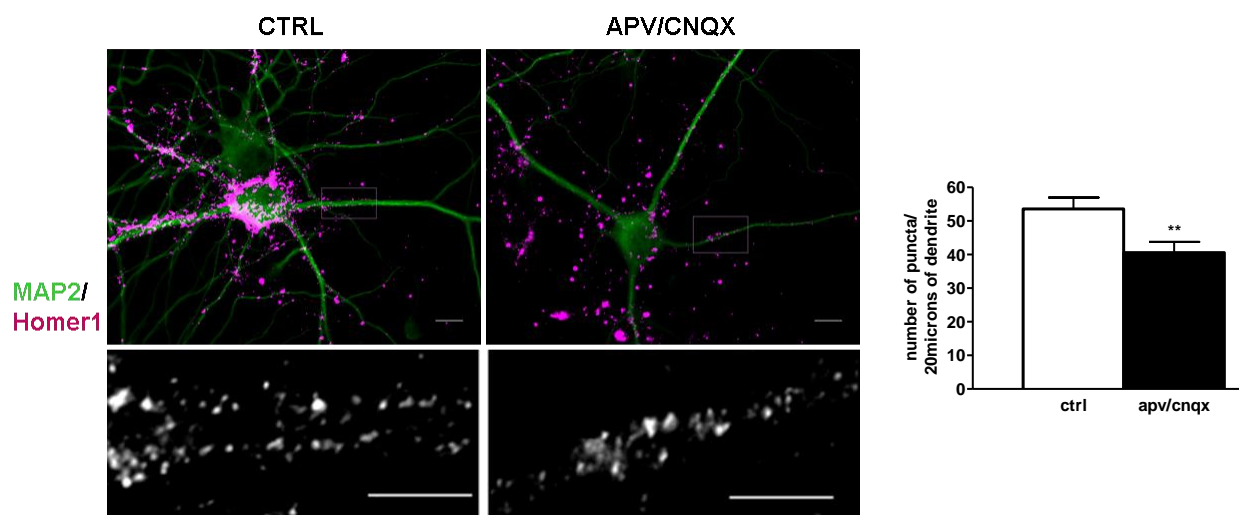


Fig. 17. Activity-dependent reduction of the postsynaptic scaffold protein Homer1. Cultured cortical neurons (21 DIV) were treated with either APV/CNQX for 48hrs or kept in control solution (CTRL). Cells were fixed, permeabilized and stained for PSD protein Homer1. Quantitative analysis showed changes in number of Homer1 puncta per 20 microns of dendrite. Scale bar, 10 microns. ** $P < 0.01$; *** $P < 0.001$ relative to control (means \pm SEM, Table 17.), t-test.

For a functional assessment of these findings electrophysiological recordings were performed in the same model system under similar experimental conditions by my colleague C. Schoene (see Appendix 1 for the results). These data revealed an increased mEPSC frequency and amplitude upon activity deprivation compared to control cells. The mEPSC frequency is thought to represent a presynaptic response to altered activity probably due to an increased vesicular release probability. Changes in the release probability might be due to changes in Ca^{2+} influx through voltage-dependent Ca^{2+} channels. To test whether an up-regulation of voltage-dependent Ca^{2+} channels contribute to this phenomena immunocytochemistry was performed using an antibody against P/Q-type Ca^{2+} . No significant differences were observed in activity-deprived vs. control cells (53.68 ± 2.514 in CTRL vs. 48.53 ± 4.09 puncta in APV/CNQX treated neurons (mean \pm SEM, $n=19$ vs. 17 cells). Puncta were counted per 20 μm of dendrite as described above) (Fig. 18.)

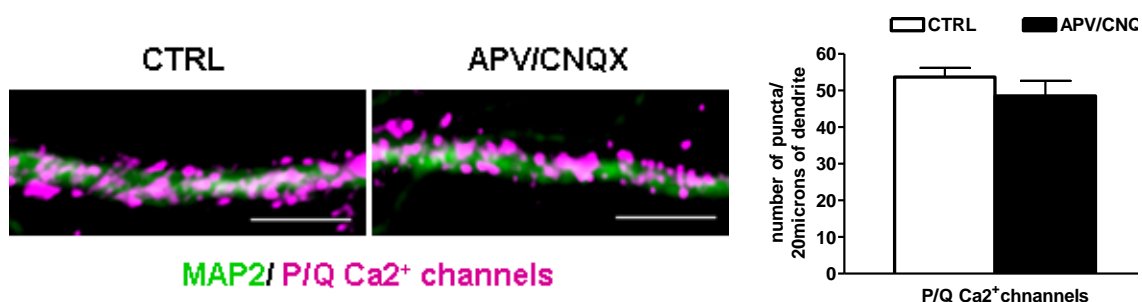


Fig. 18. No activity-dependent changes in the number of voltage-dependent Ca²⁺ channels. Activity deprived (48hrs in APV/CNQX) and contro (CTRL) cultured cortical neurons (21DIV) were stained with the antibody against P/Q-type of Ca²⁺ channels. Scale bar, 5 microns. Quantitative analysis showed no statistically significant changes in the number of protein puncta per 20 microns of dendrite from CTRL (53.68±2.514, n=19) and APV/CNQX (48.53±4.09, n=17) treated cells. Data represents the mean±SEM. t-test.

Increased mEPSC amplitude after prolonged activity blockade might be either due to accumulation of AMPA receptors at postsynaptic side or due to increased glutamate levels within SVs. Vesicular glutamate transporter (VGLUT1) is in charged for SV filling and it was already shown that VGLUT1 accumulates at synaptic site in silenced neurons (De Gois et al., 2005). Using our culture system and counting the number of VGLUT1 positive puncta in CTRL and activity deprived cells we also could show up-regulation of the VGLUT1 amount upon activity blockade (CTRL 29.55±1.519 (n=20); APV/CNQX: 35.00±1.548 (n=19); mean±SEM) (Fig.19.)

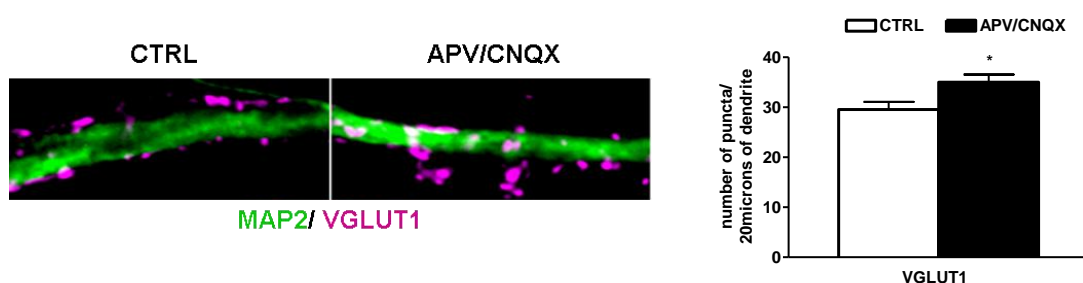


Fig. 19. Prolonged activity blockade increases the number of VGLUT1 positive puncta per 20 microns of dendrite. Control (CTRL) and activity deprived cells (APV/CNQX for 48hrs) were stained with an antibody against VGLUT1. The number of VGLUT1 positive puncta were counted along 20 microns of dendrite. Quantitative analysis showed significant upregulation of VGLUT amount upon activity blockade (CTRL 29.55±1.519 (n=20); APV/CNQX: 35.00±1.548 (n=19); mean±SEM) * P<0.05; t-test).

Taken together, the obtained results revealed that chronic inhibition of synaptic network activity reduces the global amount of CAZ proteins in silenced neurons (reduction in the total number of immunoreactive puncta). In the same neurons the amount of Bassoon, Piccolo and Munc13 proteins is also downscaled per individual synapse, as suggested by reduced fluorescence intensity measurements. In contrary, upon network

activity deprivation, the intensity of RIM immunofluorescence per individual synapse was significantly up-regulated compared to control state, suggesting that these synapses might be more active than RIMs depleted ones.

The total number of synapses measured by number of Synaptophysin positive puncta stayed unchanged upon activity deprivation, as well as, the number of immunoreactive puncta for SV proteins or P/Q-typeCa²⁺ channels. By contrast, the amount of glutamate transporter, VGLUT1, is significantly up-regulated upon activity blockade suggesting that more glutamate transporter is present on individual SVs potentially leading to higher uptake rates of the neurotransmitter.

3.2.3. Prolonged activity deprivation decreases the expression level of synaptic proteins in young cultures

Activity induced reduction of CAZ protein expression levels was also observed in younger cultures (15div) after 48h of synaptic deprivation (APV/CNQX) (Fig. 20. line 1.) compared to network activation by PTX or the control state (CTRL). Application of the Na⁺ channel blocker tetrodotoxin (2μM TTX), which also leads to silencing of the network activity by suppressing the propagation of action potentials, resulted in down-regulation of expression levels of selected proteins in the similar manner as glutamate antagonists (Fig. 20. line 3). Thus, the observed effect of downscaling of CAZ protein expression was more likely due to general changes in network activity rather than only specific effects of blocking synaptic glutamate receptor function by APV/CNQX.

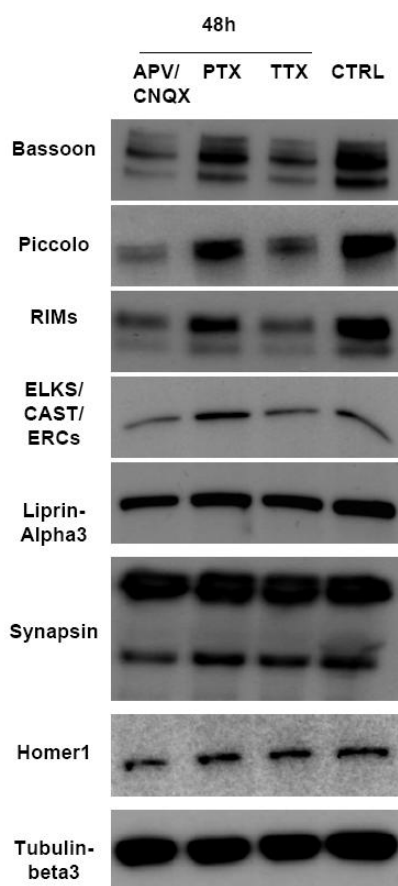


Fig. 20. Prolonged activity deprivation decreases the expression level of synaptic proteins in young cultures (15 DIV). Immunoblot analysis present changes in the expression level of selected proteins in response to prolonged activity blockade (APV/CNQX or TTX for 48h) compared to synaptic activation (PTX) or control state (CTRL). Note that overall tubulin intensity remained unchanged upon activity manipulations.

To determine the kinetics of protein profile changes in active and inactive neuronal networks, samples were prepared from the cultures of cortical neurons treated for only 24hrs with the various pharmacological agents. Quantitative analysis showed that 24hrs treatment with glutamate blocker (APV/CNQX) is not sufficient to alter the expression of synaptic proteins as it was observed after 48hrs treatment (Fig. 21.).

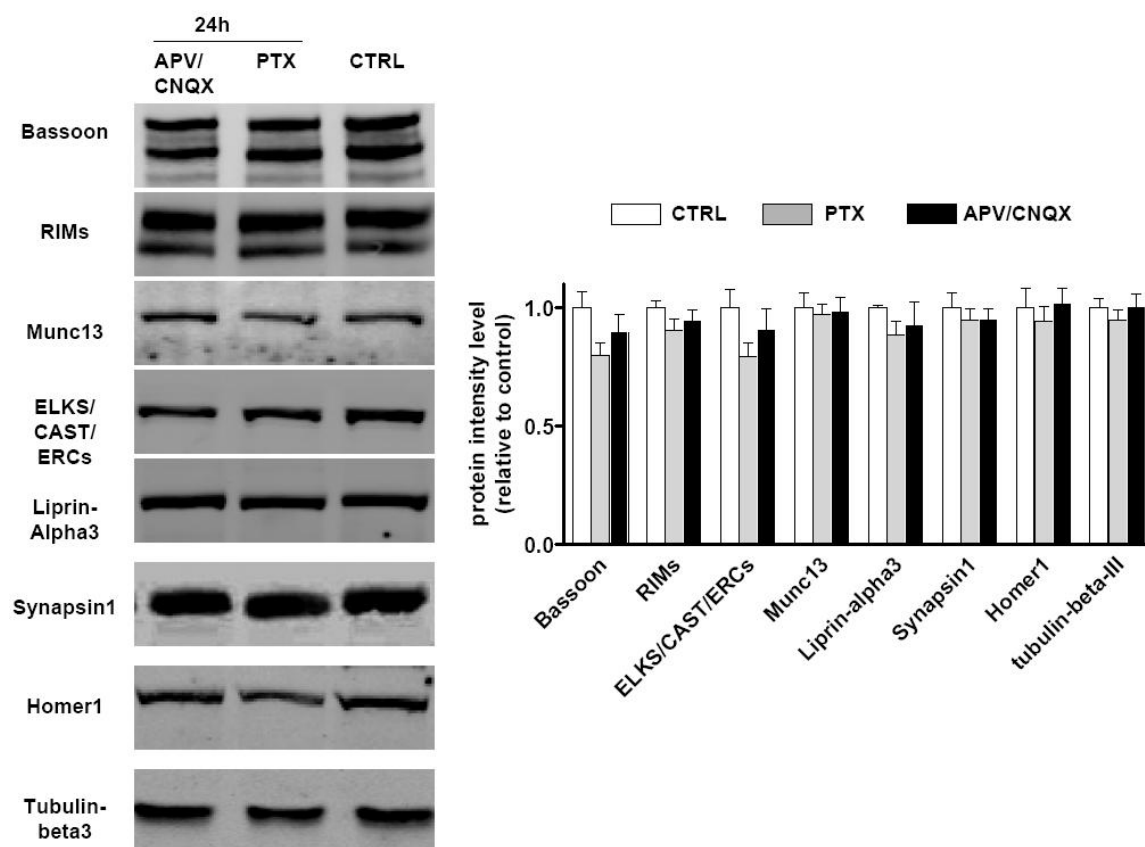


Fig. 21. Immunoblot analysis of synaptic proteins 24hrs after synaptic network deprivation (APV/CNQX) or activity enhancement (PTX). Quantification of the band intensities normalized to control values showed no significant differences of protein level expressions under different conditions (data represent means \pm SEM of the band intensities normalized to tubulin-beta3 staining, which was not changed upon activity manipulations).

3.2.4. Activity-dependent remodeling of the AZ is reversible

If alterations in the expression level of CAZ-specific proteins underlie presynaptic homeostatic plasticity during activity inhibition, then the observed changes in the molecular content of synapses in silenced neurons should be reversible after removing the drug. To test this, the basic experiment was done in the same way as above: three weeks-old cells were incubated for 48 hrs in the presence of 50 μ M APV and 10 μ M CNQX and then, for further 24hrs or 48hrs in normal medium (Fig. 22.).



Fig. 22. Scheme of the four experimental groups to test the reversibility of drug treatment. Activity inhibition in all cases was done for 48hrs (blue box). Control cells were kept in control medium all the time.

Western blot analysis showed that removing the drug leads to a visible recovery of the proteins level already after 24hrs, with an even more pronounced effect after 48hrs (Fig. 23.).

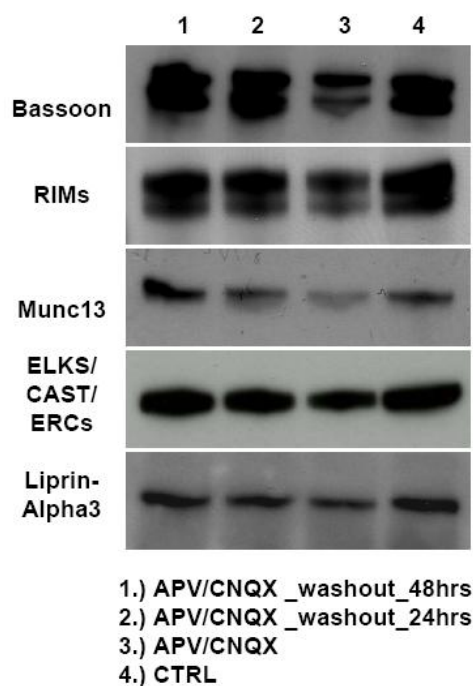


Fig. 23. Activity dependent reduction in the expression level of CAZ-specific proteins is reversible. Three weeks-old cortical neurons were incubated for 48hrs in the presence of 50 μ M APV and 10 μ M CNQX (lane 3) and then, subsequently for next 24 hrs (lane 2) or 48 hrs (lane 1) in a fresh medium without drugs. As immunoblotting revealed, washing out the drugs for 24 hrs leads already to a visible recovery of the proteins expression. The effect is much more pronounced when the washing step is 48 hrs. Control cells (lane 4, CTRL) were kept all the time in a control solution.

Therefore the quantitative immunoblot analysis was performed using the cell lysate 48hrs after the drug removal. Compared to treated cells statistically significant recovery could be observed for all CAZ proteins after 48 hrs of recovery (Bassoon, RIMs, Munc13, Liprin, CAST/ELKS/ERCs) and for postsynaptic scaffolding protein Homer 1 (Table 18, Fig. 24.).

Table 18. Percent change in protein levels after adding of APV/CNQX for 48hrs and recovery of the protein expression level 48 hrs after removing the drug

Protein	APV/CNQX_48hrs	APV/CNQX_48hrs Washout_48hrs
Bassoon	27.4 ± 2.04	62.8 ± 3.49***
RIMs	55.6 ± 5.72	83.2 ± 4.94***
Munc13	46.5 ± 9.22	64.2 ± 6.37*
Liprin_alpha3	83.6 ± 5.08	102.1 ± 0.12**
CAST/ELKS/ERCs	64.2 ± 5.40	79.33 ± 4.85*
Homer1	60.8 ± 8.44	96.57 ± 13.18**

Values indicate the percentage of the protein intensity obtained from the control (untreated) sister cultures. Data represents the mean±SEM (*P<0.05; **P<0.01; ***P<0.001; t-test)

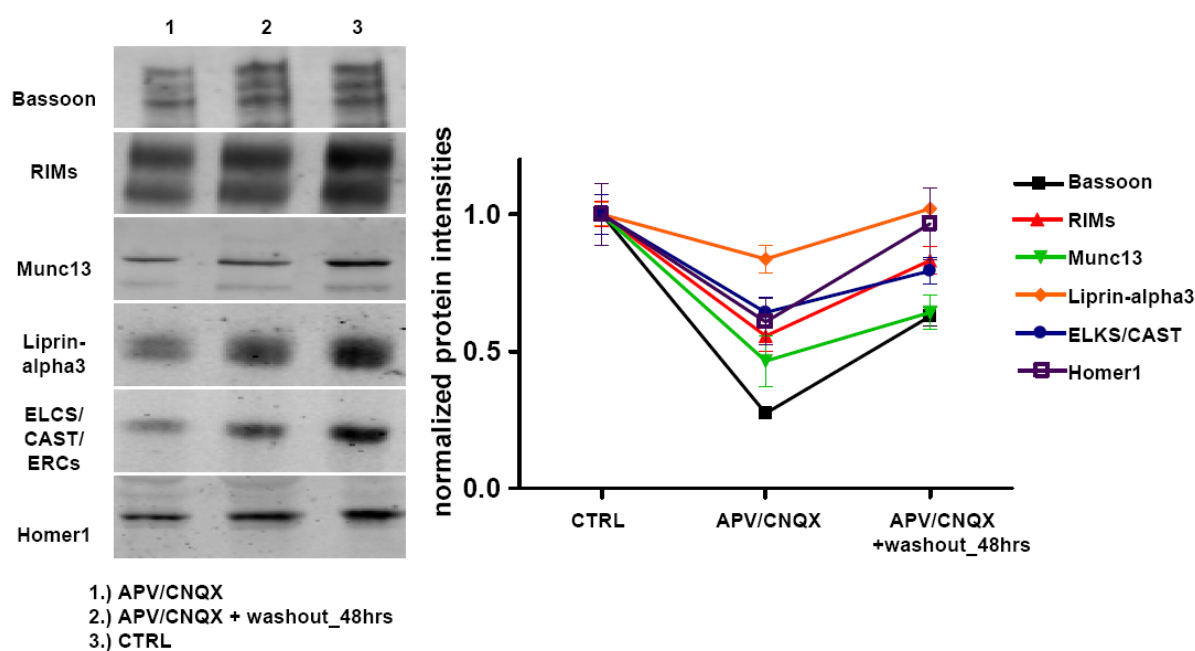


Fig. 24. Activity dependent down-regulation of selected synaptic proteins is reversible. Note significant recovery of the protein expression levels 48hrs after removing the drug from activity deprived cells (line 2) comparing to activity deprived cells (line 1). However, the protein expression level did not reach control state (line 3).

3.2.5. Activity controls protein degradation

As shown by quantitative immunoblotting and immunostaining, the amount of CAZ proteins is decreased after blockade of the excitatory transmission. Therefore we addressed the question what might be the possible molecular mechanism for the observed effects and does synaptic activity control proteasome-dependent protein degradation? To address this question we applied MG132, a potent inhibitor of proteasome-mediated protein degradation. Biochemical data indicated that inhibition of the proteasome for 6 hrs prevented activity induced decrease of CAZ proteins (Fig. 25.), suggesting that proteasome-mediated degradation might be at least one molecular mechanism underlying the activity-dependent protein turnover and global compositional changes in the presynaptic AZ.

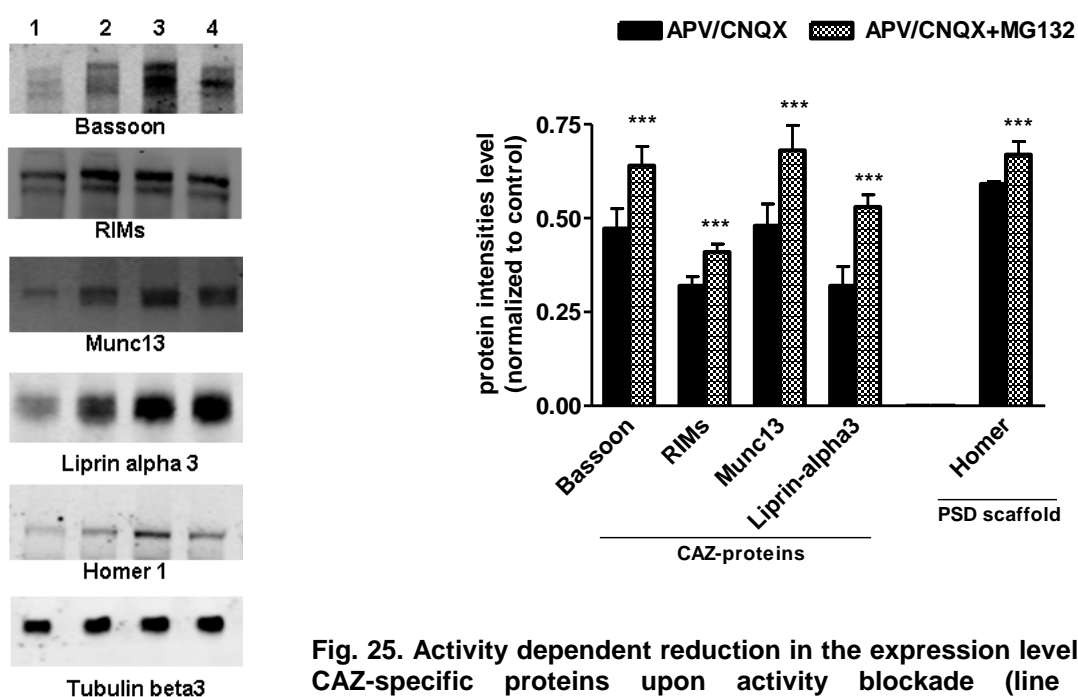


Fig. 25. Activity dependent reduction in the expression level of CAZ-specific proteins upon activity blockade (line 1. APV/CNQX for 48hrs) can be rescued by proteasome blockade. Application of MG132, a potent proteasome blocker, to activity deprived cells (line 2. APV/CNQX (48hrs) +MG132 (6hrs)) significantly increases the expression level of selected CAZ and PSD proteins. *** $P < 0.001$; t-test. However, the recovery was not to control state.

4. DISCUSSION

4.1. Ultra-structural characterization Bsn-Pclo double mutant mice

During the last decades a lot of molecular biological, biochemical and genetic studies have been performed in order to better understand mechanisms involved in processes of synaptogenesis in the central nervous system. Most likely, the specific adhesion reaction initiated by cell-cell contact between presynaptic and postsynaptic partners is the key triggering event for synapse formation, but what molecular mechanisms and signaling molecules underlie this process is still largely unknown.

In the present study, the intention was to investigate the possible role of two major presynaptic, CAZ-specific proteins, Bassoon and Piccolo, in synapse assembly and/or maturation during brain development. Both proteins are transported to the nascent synapse via 80-nm dense-core precursor vesicles called PTVs. It was shown that only 60 min after the initial cell-cell contact synapses are formed (Vardinon-Friedman et al., 2000) and both Bassoon and Piccolo are found to be in the place of newly formed synapse very early during development (Zhai et al., 2001). Based on these findings and the new observation that Bsn-Pclo double mutant animals are not viable, it was assumed that these two proteins might be important for synapse formation and/or function.

In Bsn-Pclo double deficient mice synapses are formed, as revealed by immunostaining of hippocampal cultures using anti-Synapsin antibody as synaptic marker. Synapses could also be observed at the ultrastructural level with synaptic contacts defined as sites where presynaptic boutons containing SVs are opposing postsynaptic electron dense material. Whether these synapses differ in their ultra-structure from WT synapses was one major question of the present work. To address this question conventional electron microscopy was used to examine and compare the morphology of the central synapses of cultured hippocampal neurons in the double-mutant vs. wild type animals. Previously, in work done by Altrock et al. (2003) it was shown that the absence of functional Bassoon did not alter the morphology of central synapses regarding to the length of the AZ, number of docked SVs or SV density. A detailed study on Pclo single mutant mice has not been done yet. At the first glance, however, no major phenotype could be seen. Therefore we focused our interest on double mutants first.

Electrophysiological properties of Bsn and Pclo single and Bsn-Pclo double mutant mice were studied by Alexander Meyer and Christian Rosenmund (unpublished data). Previously it was shown by Altrock et al. (2003) that loss of functional Bassoon causes a 30-50% reduction of EPSC amplitude and RRP size. The same results were obtained

from excitatory synapses of Bsn-Pclo double deficient mice. However, in inhibitory cells the size of the readily releasable pool (RRP) in Bsn single and Bsn-Pclo double mutants was reduced comparing to WT (reduction was 40%-45%), whereas in Pclo mutant mice the reduction was not significant (only 15% less than in WT neurons). The release probability did not differ between WT and Bsn mutant neurons, but in neurons lacking Pclo or in Bsn-Pclo double mutant neurons depression was slightly more pronounced than in control cells.

Comparing the features of the major presynaptic parameters between WT and Bsn-Pclo double mutant animals, we found that, although two major AZ scaffolds are missing, there is no significant difference in the ultra-structure of the presynaptic bouton between these two groups of animals. The length of the AZ (taken as a length of postsynaptic electron dense structure, the PSD), as well as total number of SV in proximal zone of the presynaptic terminal were not significantly changed in the absence of functional Bassoon and Piccolo. The number of docked SV (defined as SVs which are not more than 50 nm in distance from presynaptic plasma membrane) showed clear tendency towards reduction in double mutant mice. In three out of four animals that were analyzed the number of docked SVs was significantly down-regulated. This might be due to technical limitations using conventional EM with glutaraldehyde fixation. Aldehyde fixatives aggregate filaments (which are probably CAZ proteins and other presynaptic scaffolds) and therefore are not good for studying the ultra-structural architecture of synapses. To preserve the cytomatrix and to avoid the collapse of the presynaptic terminals, the electron tomography after high pressure freezing (HPF) of tissue can be used in order to analyze the distribution of SVs and filaments within the AZ. This method permits the discrimination of detailed morphological features such as the cytoskeleton or tethering and docking of SVs. Recently, using the HPF Siksou et al. (2009) reinvestigated the ultra-structure of Munc13 deficient mice, and by contrast to previously reported study (Varoqueaux et al., 2002) the authors found that in mutant mice SVs are not docked to the AZ plasma membrane. This finding brought the new understanding of the role of Munc13 proteins in membrane docking and functional priming of SV. Accordingly, Bsn-Pclo double mutants need to be reinvestigated in the same way.

However, counting the number of 80-nm dense-core vesicles in boutons from WT and double-mutant animals, we found a significant reduction of these structures in mutant mice. Our assumption is that PTVs constitute a major fraction of these vesicles, which serve as AZ precursor vesicles. But in the absence of the major marker proteins they cannot be identified as authentic PTVs. Previously it was shown that PTVs carry not only Bassoon and Piccolo, but also other AZ proteins that have been implicated in SV exocytosis, such as Munc13, Munc18, syntaxin, SNAP25 and N-type calcium channels

(Shapira et al., 2003). Therefore, the reduction, but not complete disappearance of “potential PTVs”, might be explained by their involvement in the delivery of these molecules to the nascent AZ during synaptogenesis. Actually our findings support the idea that multiple types of active zone transport vesicles might exist and that in the double mutant PTVs are missing. However, this hypothesis needs further attention in future.

The second important finding of the present work is a significant reduction of the thickness of PSD in Bsn-Pclo double deficient mice. The fact that mutation of two major presynaptic molecules influences the postsynaptic compartment might be surprising at the first glance. However, it is actually known that both pre- and post-synaptic compartments act synchronously during synaptogenesis in order to establish functional synapse (Fig. 26).

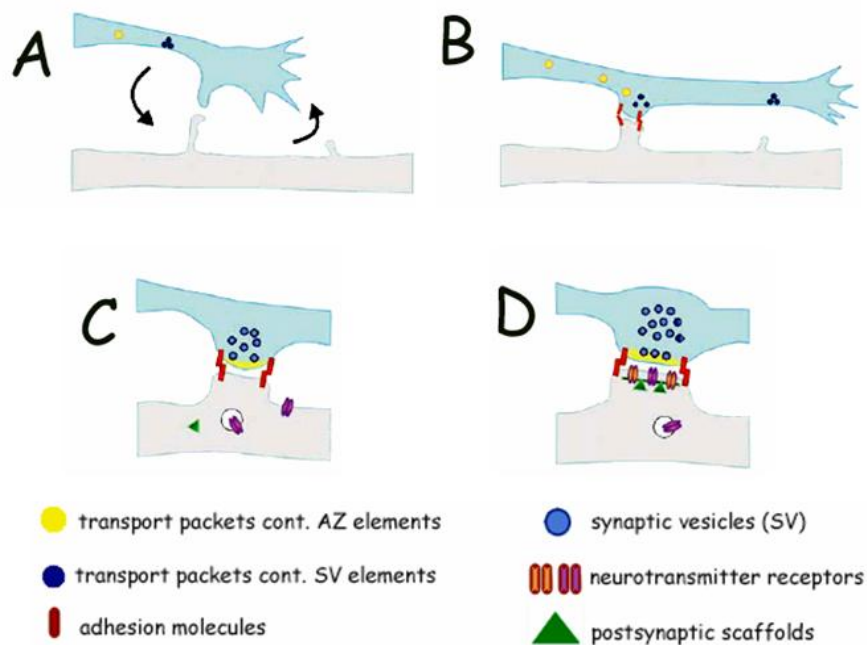


Fig. 26. Model of excitatory central synapse formation (adopted from Goda et al., 2003)

A. Early synaptogenetic signaling events involving secreted factors precede cell contact and motile filopodia search for potential partners. Neurotransmitters are released from exocytic hot spots where small clusters of synaptic vesicles are found (blue circles). Transport packets that contain active zone elements traverse along the axons (yellow circles). B. Cell adhesion molecules (red triangles) stabilize select cell contact sites. C. Active zone elements and synaptic vesicles accumulate at the presynaptic terminal. Postsynaptic terminal assembly follows presynaptic assembly by recruiting neurotransmitter receptors (double ellipses) and postsynaptic scaffolds (green triangle). D. In the assembled synapse, the presynaptic terminal has docked and reserve pool of synaptic vesicles and the postsynaptic terminal show neurotransmitter receptors embedded with the scaffold proteins.

In general, there are several possible explanations how Bassoon and Piccolo might influence PSD formation. One is that, during development, establishing of postsynaptic compartment requires mature, fully assembled presynaptic AZ, which is lacking in synapses of Bsn-Pclo double mutant mice due to absence of major AZ players.

Whether and how this is signaled to the postsynapse is not known. It is well established that interaction of presynaptic neuroligins and postsynaptic neuroligins promote the adhesion between dendrites and axons and recruitment of presynaptic and postsynaptic molecules to form a functional synapse. Therefore, the neuroligin-neurexin interaction has the ability to act as a bi-directional trigger of synapse formation (reviewed in Dean C and Dresbach T, 2006). Directly or indirectly it is possible that Bassoon and/or Piccolo as large multidomain proteins with many interaction partners regulate this interaction, which can explain why the postsynapse is not fully formed in their absence. The second hypothesis would be that 80-nm AZ precursor vesicles deliver to the nascent synapse not only AZ elements but also cell-adhesion proteins, growth factors, neurotrophins or signaling molecules, which will promote postsynaptic assembly and maturation. N-cadherin is one of the promising candidate molecules in that context, since it was shown to be important for synaptogenesis (Benson et al., 1998) and initially, N-cadherins were found on PTVs as well. Unfortunately, biochemical isolation and analysis of PTVs is a very difficult task and has not been accomplished to date. Future experiments will be necessary to gain knowledge about synapse formation and the potential role of Bassoon and Piccolo and/or other PTV components during synaptogenesis.

Recent work in our lab revealed that synaptic localization of CtBP1, a protein that is an interaction partner of Bassoon (tom Dieck, 2005, Jose et al., 2008) and probably can interact with Piccolo as well, strongly dependent on Bassoon and Piccolo (A. Fejtova, C. Schoene, unpublished). It is known that CtBPs are proteins with multiple functions including the transcriptional co-repression in the nucleus (reviewed in Chinnadurai, 2007). If the absence of Bassoon and Piccolo impaired the synaptic targeting of CtBP1 it is possible that its nuclear level rise and disturb normal transcriptional regulation including transcription of postsynaptic scaffolds. This might also explain the aberrant appearance of the PSD in double mutants. On the other hand, up-regulated CtBP1 in the nucleus might alter the epigenetic state of chromatin, since CtBP1 also has been shown to recruit HDACs (histone deacetylases) (Subramanian, 2003) and that might cause early neonatal lethality of Bsn-Pclo double mutant animals.

Based on the data described here, we can assume that Bassoon and Piccolo, although the major constituents of the AZs present in the synapses very early during development, are not essential for synapse formation *per se*. Since, their absence influences the postsynaptic formation we can conclude that both, Bassoon and Piccolo are important for synapse maturation and therefore for establishment of the functional synaptic contacts. Function of synapses formed in the absence of these two proteins is not compatible with life causing early neonatal lethality of Bsn-Pclo double mutant animals.

4.2. Activity dependent remodelling of the AZ

Homeostatic plasticity and synaptic scaling are concepts used to describe the modifications that neurons undergo while adapting to persistent alternations in input strength. The cellular mechanisms underlying these forms of plasticity are still poorly understood and for a long time the question whether the expression locus of homeostatic plasticity is presynaptic or postsynaptic was controversial. Work done by Wierenga et al. (2006) shed new light on this issue providing evidence that there is a developmental switch in the expression locus, from purely postsynaptic response in young neurons to mixed pre- and postsynaptic response in older ones. In case of activity deprivation, presynaptic response is represented as increased mEPSC frequency and postsynaptic response is assessed as increased mEPSC amplitude (Turrigiano et al., 1998). Increased mEPSC frequency is assumed to be driven by presynaptic modifications of release properties (i.e. probability of SV release), whereas changes in the amplitude are underlined by receptor accumulation at postsynaptic site (O'Brien et al., 1998) or by changes in the glutamate filling into SVs (Wilson et al. 2005).

In the present study we have investigated whether and how the altered synaptic network activity influences the molecular composition of presynaptic AZ. Also, we wanted to address the question what might be possible mechanism underlying activity-dependent AZ remodelling.

Using cortical neurons as a convenient and well established model system accessible for various activity-dependent manipulations we could show that prolonged network activity deprivation in three weeks old cultures exerted significant down-regulation of the expression level of all CAZ-specific proteins (Bassoon, Piccolo, Munc13, RIMs, Liprin-alphas) as well as the presynaptic scaffolding protein Synapsin. Interestingly, the same condition did not alter the expression level of SV (SV2B and Synaptophysin) and SNARE family proteins (Syntaxins), and moreover, we were able to confirm in our experimental setup previously reported downscaling of some of the PSD scaffolding proteins (PSD-95, Homer) (Ehlers, 2003). By contrast to activity deprivation, further excitation of synaptic activity, by blocking inhibitory GABA_A receptors, did not alter protein composition as compared to the control state. This might be explained, at least partially, by already high level of basal activity in our culture system due to high density of plated cells (300.000/well).

To distinguish whether the observed downscaling of CAZ-associated proteins during synaptic blockade is due to reduced amount of these proteins in all synapses or due to reduced total number of synapses in activity deprived neurons, we applied an immunocytochemical approach. The data revealed that, in spite of deprived synaptic

network activity, the overall number of synapses is not changed. However, the number of synaptic puncta stained with antibody against different CAZ proteins (Bassoon, Piccolo, RIMs, Munc13) was significantly reduced. Very interestingly, the intensity of RIM fluorescence in individual synapse was significantly up-regulated compared to the control state, in contrast to Bassoon, Piccolo and Munc13 whose intensities per synapse were reduced upon network activity deprivation. Since the expression levels of RIMs are down-regulated and the total number of RIM-positive puncta is significantly reduced in silenced neurons, the measurements of the RIM fluorescence intensity suggest that a subpopulation of synapses with enhanced RIM fluorescence upon activity deprivation might become more active in comparison with RIM-depleted ones. Labeling of active synapses in living cells using the antibody against luminal domain of synaptic vesicle protein Synaptotagmin and subsequent double staining with RIMs antibody should help to clarify this point in future experiments. Also, comparing the total number of active synapses and/or the ratio between total number of synapses (using Synaptophysin antibody as a synaptic marker) and the active ones will gain the new insights for the understanding of how global network activity deprivation modulates synaptic transmission at single synapses.

To provide physiological relevance for the present data electrophysiological recordings were performed to measure the synaptic strength in the same model system and under same conditions that were used for biochemical and immunocytochemical approach (Schöne, 2009, diploma thesis). Increased synaptic strength, assessed by measuring amplitudes and frequencies of mEPSC, upon chronic network activity blockade has been already well documented (Turrigiano et al., 1998; O'Brien et al., 1998; Bacci et al., 2001; Galvan et al., 2003). In our experimental setup we could confirm previously reported findings that prolonged network activity blockade increases both, mEPSC amplitude and frequency (C. Schoene, 2009; see Fig. S1 of appendix 1). As increased mEPSC amplitude might indicate changes in the glutamate filling into SVs, we have looked for the amount of the glutamate transporter (VGLUT1), which is in charged for SVs filling. The data confirmed an accumulation of VGLUT1 at synaptic sites upon network activity blockade comparing to control state, which is in agreement with published results of De Gois et al. (2005).

An increase of mEPSC frequency, as a presynaptic response to neuronal activity blockade, is believed to reflect an enhancement of SV release probability. Analysing the ultra-structure of hippocampal synapses upon prolonged activity deprivation, Murthy et al. (2001) showed an increase in AZ length, PSD and volume of presynaptic bouton. In parallel with anatomical changes, the physiologically measured size of the RRP and the release probability were also increased. Since, physiologically defined RRP correlates

with the docked vesicle pool, the authors could also observe an enhanced number of docked SV in silenced neurons. The possible mechanism underlying increased release probability can include CaMKII- (Ca^{2+} -Calmodulin-dependent protein kinase II-) dependent phosphorylation of Synapsin. CaMKII is shown to be negatively regulated by Piccolo and since we could show that Piccolo is down-regulated after activity deprivation, CaMKII can increase the phosphorylation of Synapsin which then accelerates SV exocytosis by enhancing Synapsin dispersion and mobility (Leal-Ortiz, 2008; Coleman and Bykhovskaia, 2009). We found an overall reduction of Synapsin in silenced neurons, but whether there is activity-dependent increase in the amount of phosphorylated ones might be assessed by immunoblotting using phosphospecific anti-Synapsin antibody. Changes in the probability of release are also known to be mediated by changes in the Ca^{2+} entry through P/Q-type Ca^{2+} channels. Our data showed no significant differences in the amount of these channels per synapse, but whether there is a change in Ca^{2+} influx upon activity blockade might be further investigated by recording whole-cell calcium currents and comparing it to control cells.

Recently, Ibata et al. (2008) showed that drop in Ca^{2+} influx triggers scaling up of synaptic strength via signal that leads to increase in AMPA receptors at synaptic site. Ca^{2+} influx can be sensed by different calcium-dependent protein kinases (CaMKs) and CaMKIV is one of the family members that might be involved in synaptic scaling (Ibata et al., 2008). CaMKIV has a strong nuclear localization and acts there as transcriptional regulator. Under normal conditions CaMKIV is highly activated but network activity blockade reduces the pool of active kinases and that might influence the expression of factors that will in turn enhance synaptic accumulation of AMPA receptors.

The role of CAZ-associated proteins in increased release probability upon activity blockade might be viewed also from the side of CAZ proteins as spatial organisers of the AZ, a place where neurotransmission occurs. CAZ proteins are thought to make a grid or a web-like platform within the AZ, which keeps the SVs in a close proximity to the fusion machinery and presynaptic plasma membrane where the exocytosis will take a place. SVs within the presynaptic terminal are not functionally identical and they belong to different pools of vesicles, either to reserve (resting) pool or to recycling pool (reviewed in Gundelfinger et al., 2003). A subpopulation of the vesicles from recycling pool is tethered to presynaptic plasma membrane and primed for fusion step and those SV represent RRP. If activity blockade reduces the amount of all CAZ proteins as our data showed, than the grid becomes weaker and not able anymore to hold SVs in proper order. More SVs might move from reserve to the RRP and therefore enhance the probability of release.

Activity-dependent changes in the molecular content of the silenced AZs are reversible, giving further physiological relevance to the observed phenomena. We could show that removing of the receptor blockers leads to a visible recovery of the CAZ proteins level already after 24h, with an even more significant effect after 48h, as compared to activity-deprived neurons, but without full recovery to control state. Electrophysiological recordings performed in the same system, showed reversed mEPSC amplitude after drugs were washed out for 48hrs, but the frequency did not reverse (C. Schoene, 2009; see appendix 1, Figs. S2 and S3). This later observation can be explained by the fact that probably only fully established presynaptic grid made by CAZ proteins might properly regulate SVs release. Since 48hrs after the drugs were washed out the CAZ proteins level did not reach the control state, the release probability might stay still high and cause the enhanced frequency.

4.2.1. Potential role of the ubiquitin-proteasome system in homeostatic plasticity

The data presented above demonstrate an activity-dependent modulation of neurotransmitter release and activity-dependent involvement of CAZ proteins in this process. The neurotransmission can be regulated by modifying the composition of proteins which are involved in SV cycle, by activity-dependent synthesis, degradation or activity-dependent posttranslational modifications.

The ubiquitin-proteasome system (UPS) is emerging as a powerful modulator of synaptic function, acting at both, postsynaptic and presynaptic sites. Ehlers (2003) could show that activity-dependent changes in PSD require ubiquitin-proteasome-mediated degradation. Colledge et al. (2003) described a proteasomal-target model in which postsynaptic scaffold, PSD-95, is rapidly ubiquitinated in response to NMDA-receptor activation and Saliba et al. (2007) showed that chronic blockade of neuronal activity dramatically increases the level of GABA_A receptor ubiquitination and its subsequent proteasomal degradation. That proteasoms can modulate synaptic transmission presynaptically was shown at *Drosophyla* NMJ (Aravamudan and Broady, 2003) and in the *Aplysia* sensory-motor synapse (Zhao et al., 2003). In *Drosophila* this regulation appears to be dependent on the activity of protein kinase A (PKA) and includes Dunc13 protein (*Drosophila's* only homologue of mammalian Munc13s) which is involved in vesicle priming. Proteasome inhibition at the *Drosophila* NMJ increased the level of Dunc13 protein and this effect could be abolished by PKA antagonists (Aravamudan and Broady, 2003). Furthermore, in cultured hippocampal neurons, it was shown that proteasome inhibition triggers activity-dependent increase in the size of recycling vesicle pool through

the mechanism that probably involves PKA. Activation of cAMP-PKA pathway is capable of recruiting vesicles to the RRP, but in the presence of proteasome inhibitors the PKA pathway does not further modulate the vesicle recycling pool (Willeumier et al., 2006).

Taken together, activity-dependent protein degradation appears as a new mechanism, apart of gene transcription and translation strongly contributing to the homeostatic plasticity.

In our study we could show that activity-induced proteasomal degradation might be a mechanism underlying observed downscaling of CAZ proteins as well. The effect of activity deprivation which leads to downscaling of the CAZ-associated proteins might be partially rescued by proteasomal inhibition. Six hrs after proteasomal inhibition of activity deprived cells we could observe significant (comparing to silenced cells) but not full recovery (comparing to control cells) of all CAZ proteins.

Again the physiological relevance of the obtained data was assessed by electrophysiological recordings (appendix 1, Figs. S2 and S3). Interestingly, although MG132 treatment did not affect mean amplitudes of control cells, activity deprived cells treated with MG132 showed further increases of mEPSC amplitude compared to control cells. This suggests that there must be an activity-dependent modification (maybe ubiquitination) of AMPA receptors which, since the proteasomes are blocked, will not undergo degradation but will be recycled or their internalization from the postsynaptic membrane will be reduced and more receptors will stay at the surface available for neurotransmitters contributing to enhanced amplitude.

The mEPSC frequency of activity deprived neurons upon proteasome inhibition is significantly higher than in control cells. This might be explained by insufficient recovery of CAZ proteins upon proteasome blockade of silenced neurons (since the protein levels did not reach control state) and therefore a still high rate of SV release. MG132 treatment of control cells also significantly increased frequency compared to control condition, probably accumulating other molecules (apart from the CAZ) involved in neurotransmitter release. Further investigation should address the question which of the proteins involved in SV cycle are upregulated upon proteasome inhibition. Obtained data suggested that pre- and postsynaptic compartment behaving differently upon proteasomal inhibition and activity state of the system plays an important role in this process. This further places the activity-dependent protein degradation as an important mechanism during homeostatic plasticity.

The experiment with proteasomal inhibitors also raised a question regarding to activity-dependent protein synthesis that was not investigated in this study. According to our data, activity deprivation down-regulates the expression of CAZ proteins, which then can be rescued by blocking of proteasomes. This suggests a higher degradation rate of CAZ proteins upon activity blockade. Whether activity-deprivation alters global protein

turnover can be measured using ^{35}S -cysteine/methionine metabolic labeling pulse-chase analysis.

Taken together our data revealed that chronic modulation of global network activity alter synaptic strength and CAZ proteins might contribute to the presynaptic homeostatic plasticity by downscaling of the expression level during activity deprivation. The effect is reversible and involves the ubiquitin-proteasome system. Interestingly, all CAZ proteins showed similar pattern of behavior upon different activity manipulations. This implies that at the active zone CAZ proteins really exist as functional and/or physiological ensembles (grid), although each protein has its unique and specific function as well. On the other hand, this resemblance in the activity-induced behavior of CAZ proteins suggests that control over composition of CAZ may be governed by the incorporation or removal of certain “scaling molecules” that preserve stoichiometric relationships between CAZ proteins. A similar paradigm exists at the postsynaptic site, regarding the activity-induced composition of PSD proteins (Ehlers, 2003). The nature of these “scaling molecules” remains to be discovered. They might be e.g. E3 ligases promoting ubiquitination of proteins and their targeting to the activity-dependent proteasomal degradation, but also they might be some signaling molecules, which are produced by the postsynapse and act retrogradely on presynaptic plasma membrane, since it is still unclear how exactly glutamate receptor blockade generates a modulation of the presynaptic properties.

We believe that our study brought new insights into understanding the basic processes that undergo in activity dependent manner and especially how the presynaptic AZ might contribute to the homeostatic plasticity. That is very important issue because homeostatic processes are basis for normal neuronal network functioning during development, plastic changes underlying learning and memory, but also, during different neuropathies and pathological conditions.

5. LITERATURE

- Ahmari, S.E., Buchanan, J., and Smith, S.J. (2000). Assembly of presynaptic active zones from cytoplasmic transport packets. *Nat Neurosci* 3, 445-451.
- Altmann, W.D., tom Dieck, S., Sokolov, M., Meyer, A.C., Sigler, A., Brakebusch, C., Fassler, R., Richter, K., Boeckers, T.M., Potschka, H., et al. (2003). Functional inactivation of a fraction of excitatory synapses in mice deficient for the active zone protein bassoon. *Neuron* 37, 787-800.
- Angenstein, F., Hilfert, L., Zuschratter, W., Altmann, W.D., Niessen, H.G., and Gundelfinger, E.D. (2008). Morphological and metabolic changes in the cortex of mice lacking the functional presynaptic active zone protein bassoon: a combined ¹H-NMR spectroscopy and histochemical study. *Cereb Cortex* 18, 890-897.
- Aravamudan, B., and Broadie, K. (2003). Synaptic *Drosophila* UNC-13 is regulated by antagonistic G-protein pathways via a proteasome-dependent degradation mechanism. *J Neurobiol* 54, 417-438.
- Bacci, A., Coco, S., Pravettoni, E., Schenk, U., Armano, S., Frassoni, C., Verderio, C., De Camilli, P., and Matteoli, M. (2001). Chronic blockade of glutamate receptors enhances presynaptic release and downregulates the interaction between synaptophysin-synaptobrevin-vesicle-associated membrane protein 2. *J Neurosci* 21, 6588-6596.
- Banker, G., and Goslin, K. (1988). Developments in neuronal cell culture. *Nature* 336, 185-186.
- Benson, D.L., and Tanaka, H. (1998). N-cadherin redistribution during synaptogenesis in hippocampal neurons. *J Neurosci* 18, 6892-6904.
- Betz, A., Ashery, U., Rickmann, M., Augustin, I., Neher, E., Sudhof, T.C., Rettig, J., and Brose, N. (1998). Munc13-1 is a presynaptic phorbol ester receptor that enhances neurotransmitter release. *Neuron* 21, 123-136.
- Betz, A., Thakur, P., Junge, H.J., Ashery, U., Rhee, J.S., Scheuss, V., Rosenmund, C., Rettig, J., and Brose, N. (2001). Functional interaction of the active zone proteins Munc13-1 and RIM1 in synaptic vesicle priming. *Neuron* 30, 183-196.
- Calakos, N., Schoch, S., Sudhof, T.C., and Malenka, R.C. (2004). Multiple roles for the active zone protein RIM1alpha in late stages of neurotransmitter release. *Neuron* 42, 889-896.

- Cases-Langhoff, C., Voss, B., Garner, A.M., Appeltauer, U., Takei, K., Kindler, S., Veh, R.W., De Camilli, P., Gundelfinger, E.D., and Garner, C.C. (1996). Piccolo, a novel 420 kDa protein associated with the presynaptic cytomatrix. *Eur J Cell Biol* 69, 214-223.
- Chinnadurai, G. (2007). Transcriptional regulation by C-terminal binding proteins. *Int J Biochem Cell Biol* 39, 1593-1607.
- Coleman, W.L., and Bykhovskaia, M. (2009). Synapsin I accelerates the kinetics of neurotransmitter release in mouse motor terminals. *Synapse* 63, 531-533.
- Colledge, M., Snyder, E.M., Crozier, R.A., Soderling, J.A., Jin, Y., Langeberg, L.K., Lu, H., Bear, M.F., and Scott, J.D. (2003). Ubiquitination regulates PSD-95 degradation and AMPA receptor surface expression. *Neuron* 40, 595-607.
- De Gois, S., Schafer, M.K., Defamie, N., Chen, C., Ricci, A., Weihe, E., Varoqui, H., and Erickson, J.D. (2005). Homeostatic scaling of vesicular glutamate and GABA transporter expression in rat neocortical circuits. *J Neurosci* 25, 7121-7133.
- Dean, C., and Dresbach, T. (2006). Neuroligins and neuexins: linking cell adhesion, synapse formation and cognitive function. *Trends Neurosci* 29, 21-29.
- Dick, O., tom Dieck, S., Altmann, W.D., Ammermuller, J., Weiler, R., Garner, C.C., Gundelfinger, E.D., and Brandstatter, J.H. (2003). The presynaptic active zone protein bassoon is essential for photoreceptor ribbon synapse formation in the retina. *Neuron* 37, 775-786.
- Dresbach, T., Torres, V., Wittenmayer, N., Altmann, W.D., Zamorano, P., Zuschratter, W., Nawrotzki, R., Ziv, N.E., Garner, C.C., and Gundelfinger, E.D. (2006). Assembly of active zone precursor vesicles: obligatory trafficking of presynaptic cytomatrix proteins Bassoon and Piccolo via a trans-Golgi compartment. *J Biol Chem* 281, 6038-6047.
- Ehlers, M.D. (2003). Activity level controls postsynaptic composition and signaling via the ubiquitin-proteasome system. *Nat Neurosci* 6, 231-242.
- Fejtova, A., Davydova, D., Bischof, F., Lazarevic, V., Altmann, W.D., Romorini, S., Schone, C., Zuschratter, W., Kreutz, M.R., Garner, C.C., et al. (2009). Dynein light chain regulates axonal trafficking and synaptic levels of Bassoon. *J Cell Biol* 185, 341-355.
- Fenster, S.D., Chung, W.J., Zhai, R., Cases-Langhoff, C., Voss, B., Garner, A.M., Kaempf, U., Kindler, S., Gundelfinger, E.D., and Garner, C.C. (2000). Piccolo, a presynaptic zinc finger protein structurally related to bassoon. *Neuron* 25, 203-214.
- Fenster, S.D., Kessels, M.M., Qualmann, B., Chung, W.J., Nash, J., Gundelfinger, E.D., and Garner, C.C. (2003). Interactions between Piccolo and the

- actin/dynamin-binding protein Abp1 link vesicle endocytosis to presynaptic active zones. *J Biol Chem* 278, 20268-20277.
- Fouquet, W., Oswald, D., Wichmann, C., Mertel, S., Depner, H., Dyba, M., Hallermann, S., Kittel, R.J., Eimer, S., and Sigrist, S.J. (2009). Maturation of active zone assembly by *Drosophila* Bruchpilot. *J Cell Biol* 186, 129-145.
 - Friedman, H.V., Bresler, T., Garner, C.C., and Ziv, N.E. (2000). Assembly of new individual excitatory synapses: time course and temporal order of synaptic molecule recruitment. *Neuron* 27, 57-69.
 - Galvan, C.D., Wenzel, J.H., Dineley, K.T., Lam, T.T., Schwartzkroin, P.A., Sweatt, J.D., and Swann, J.W. (2003). Postsynaptic contributions to hippocampal network hyperexcitability induced by chronic activity blockade in vivo. *Eur J Neurosci* 18, 1861-1872.
 - Ghiglieri, V., Picconi, B., Sgobio, C., Bagetta, V., Barone, I., Paille, V., Di Filippo, M., Polli, F., Gardoni, F., Altmann, W., et al. (2009). Epilepsy-induced abnormal striatal plasticity in Bassoon mutant mice. *Eur J Neurosci* 29, 1979-1993.
 - Goda, Y., and Davis, G.W. (2003). Mechanisms of synapse assembly and disassembly. *Neuron* 40, 243-264.
 - Gundelfinger, E.D., Kessels, M.M., and Qualmann, B. (2003). Temporal and spatial coordination of exocytosis and endocytosis. *Nat Rev Mol Cell Biol* 4, 127-139.
 - Ibata, K., Sun, Q., and Turrigiano, G.G. (2008). Rapid synaptic scaling induced by changes in postsynaptic firing. *Neuron* 57, 819-826.
 - Jose, M., Nair, D.K., Altmann, W.D., Dresbach, T., Gundelfinger, E.D., and Zuschratter, W. (2008). Investigating interactions mediated by the presynaptic protein bassoon in living cells by Foerster's resonance energy transfer and fluorescence lifetime imaging microscopy. *Biophys J* 94, 1483-1496.
 - Khimich, D., Nouvian, R., Pujol, R., Tom Dieck, S., Egner, A., Gundelfinger, E.D., and Moser, T. (2005). Hair cell synaptic ribbons are essential for synchronous auditory signalling. *Nature* 434, 889-894.
 - Kim, J.H., and Haganir, R.L. (1999). Organization and regulation of proteins at synapses. *Curr Opin Cell Biol* 11, 248-254.
 - Kirov, S.A., and Harris, K.M. (1999). Dendrites are more spiny on mature hippocampal neurons when synapses are inactivated. *Nat Neurosci* 2, 878-883.
 - Kreienkamp, H.J. (2008). Scaffolding proteins at the postsynaptic density: shank as the architectural framework. *Handb Exp Pharmacol*, 365-380.

- Leal-Ortiz, S., Waites, C.L., Terry-Lorenzo, R., Zamorano, P., Gundelfinger, E.D., and Garner, C.C. (2008). Piccolo modulation of Synapsin1a dynamics regulates synaptic vesicle exocytosis. *J Cell Biol* 181, 831-846.
- Lonart, G., Schoch, S., Kaeser, P.S., Larkin, C.J., Sudhof, T.C., and Linden, D.J. (2003). Phosphorylation of RIM1alpha by PKA triggers presynaptic long-term potentiation at cerebellar parallel fiber synapses. *Cell* 115, 49-60.
- Lu, Y.M., Mansuy, I.M., Kandel, E.R., and Roder, J. (2000). Calcineurin-mediated LTD of GABAergic inhibition underlies the increased excitability of CA1 neurons associated with LTP. *Neuron* 26, 197-205.
- Murthy, V.N., Schikorski, T., Stevens, C.F., and Zhu, Y. (2001). Inactivity produces increases in neurotransmitter release and synapse size. *Neuron* 32, 673-682.
- O'Brien, R.J., Kamboj, S., Ehlers, M.D., Rosen, K.R., Fischbach, G.D., and Huganir, R.L. (1998). Activity-dependent modulation of synaptic AMPA receptor accumulation. *Neuron* 21, 1067-1078.
- Ohtsuka, T., Takao-Rikitsu, E., Inoue, E., Inoue, M., Takeuchi, M., Matsubara, K., Deguchi-Tawarada, M., Satoh, K., Morimoto, K., Nakanishi, H., et al. (2002). Cast: a novel protein of the cytomatrix at the active zone of synapses that forms a ternary complex with RIM1 and munc13-1. *J Cell Biol* 158, 577-590.
- Okabe, S. (2007). Molecular anatomy of the postsynaptic density. *Mol Cell Neurosci* 34, 503-518.
- Powell, C.M., Schoch, S., Monteggia, L., Barrot, M., Matos, M.F., Feldmann, N., Sudhof, T.C., and Nestler, E.J. (2004). The presynaptic active zone protein RIM1alpha is critical for normal learning and memory. *Neuron* 42, 143-153.
- Richter, K., Langnaese, K., Kreutz, M.R., Olias, G., Zhai, R., Scheich, H., Garner, C.C., and Gundelfinger, E.D. (1999). Presynaptic cytomatrix protein bassoon is localized at both excitatory and inhibitory synapses of rat brain. *J Comp Neurol* 408, 437-448.
- Rizo, J., and Rosenmund, C. (2008). Synaptic vesicle fusion. *Nat Struct Mol Biol* 15, 665-674.
- Rosenmund, C., Rettig, J., and Brose, N. (2003). Molecular mechanisms of active zone function. *Curr Opin Neurobiol* 13, 509-519.
- Saliba, R.S., Michels, G., Jacob, T.C., Pangalos, M.N., and Moss, S.J. (2007). Activity-dependent ubiquitination of GABA(A) receptors regulates their accumulation at synaptic sites. *J Neurosci* 27, 13341-13351.
- Schmitz, F., Konigstorfer, A., and Sudhof, T.C. (2000). RIBEYE, a component of synaptic ribbons: a protein's journey through evolution provides insight into synaptic ribbon function. *Neuron* 28, 857-872.

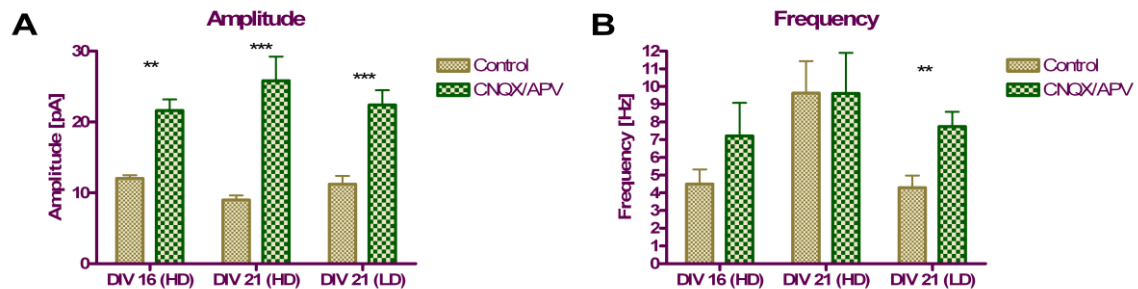
- Schoch, S., and Gundelfinger, E.D. (2006). Molecular organization of the presynaptic active zone. *Cell Tissue Res* 326, 379-391.
- Serra-Pages, C., Kedersha, N.L., Fazikas, L., Medley, Q., Debant, A., and Streuli, M. (1995). The LAR transmembrane protein tyrosine phosphatase and a coiled-coil LAR-interacting protein co-localize at focal adhesions. *EMBO J* 14, 2827-2838.
- Shapira, M., Zhai, R.G., Dresbach, T., Bresler, T., Torres, V.I., Gundelfinger, E.D., Ziv, N.E., and Garner, C.C. (2003). Unitary assembly of presynaptic active zones from Piccolo-Bassoon transport vesicles. *Neuron* 38, 237-252.
- Shin, H., Wyszynski, M., Huh, K.H., Valtschanoff, J.G., Lee, J.R., Ko, J., Streuli, M., Weinberg, R.J., Sheng, M., and Kim, E. (2003). Association of the kinesin motor KIF1A with the multimodular protein liprin-alpha. *J Biol Chem* 278, 11393-11401.
- Siksou, L., Rostaing, P., Lechaire, J.P., Boudier, T., Ohtsuka, T., Fejtova, A., Kao, H.T., Greengard, P., Gundelfinger, E.D., Triller, A., et al. (2007). Three-dimensional architecture of presynaptic terminal cytomatrix. *J Neurosci* 27, 6868-6877.
- Siksou, L., Triller, A., and Marty, S. (2009). An emerging view of presynaptic structure from electron microscopic studies. *J Neurochem* 108, 1336-1342.
- Siksou, L., Varoqueaux, F., Pascual, O., Triller, A., Brose, N., and Marty, S. (2009). A common molecular basis for membrane docking and functional priming of synaptic vesicles. *Eur J Neurosci* 30, 49-56.
- Spangler, S.A., and Hoogenraad, C.C. (2007). Liprin-alpha proteins: scaffold molecules for synapse maturation. *Biochem Soc Trans* 35, 1278-1282.
- Subramanian, T., and Chinnadurai, G. (2003). Association of class I histone deacetylases with transcriptional corepressor CtBP. *FEBS Lett* 540, 255-258.
- Takao-Rikitsu, E., Mochida, S., Inoue, E., Deguchi-Tawarada, M., Inoue, M., Ohtsuka, T., and Takai, Y. (2004). Physical and functional interaction of the active zone proteins, CAST, RIM1, and Bassoon, in neurotransmitter release. *J Cell Biol* 164, 301-311.
- tom Dieck, S., Altroch, W.D., Kessels, M.M., Qualmann, B., Regus, H., Brauner, D., Fejtova, A., Bracko, O., Gundelfinger, E.D., and Brandstatter, J.H. (2005). Molecular dissection of the photoreceptor ribbon synapse: physical interaction of Bassoon and RIBEYE is essential for the assembly of the ribbon complex. *J Cell Biol* 168, 825-836.
- tom Dieck, S., Sanmarti-Vila, L., Langnaese, K., Richter, K., Kindler, S., Soyke, A., Wex, H., Smalla, K.H., Kampf, U., Franzer, J.T., et al. (1998). Bassoon, a novel

- zinc-finger CAG/glutamine-repeat protein selectively localized at the active zone of presynaptic nerve terminals. *J Cell Biol* 142, 499-509.
- Tsuritel, S., Geva, R., Zamorano, P., Dresbach, T., Boeckers, T., Gundelfinger, E.D., Garner, C.C., and Ziv, N.E. (2006). Local sharing as a predominant determinant of synaptic matrix molecular dynamics. *PLoS Biol* 4, e271.
 - Turrigiano, G. (2007). Homeostatic signaling: the positive side of negative feedback. *Curr Opin Neurobiol* 17, 318-324.
 - Turrigiano, G.G., Leslie, K.R., Desai, N.S., Rutherford, L.C., and Nelson, S.B. (1998). Activity-dependent scaling of quantal amplitude in neocortical neurons. *Nature* 391, 892-896.
 - Varoqueaux, F., Sigler, A., Rhee, J.S., Brose, N., Enk, C., Reim, K., and Rosenmund, C. (2002). Total arrest of spontaneous and evoked synaptic transmission but normal synaptogenesis in the absence of Munc13-mediated vesicle priming. *Proc Natl Acad Sci U S A* 99, 9037-9042.
 - Wagh, D.A., Rasse, T.M., Asan, E., Hofbauer, A., Schwenkert, I., Durrbeck, H., Buchner, S., Dabauvalle, M.C., Schmidt, M., Qin, G., et al. (2006). Bruchpilot, a protein with homology to ELKS/CAST, is required for structural integrity and function of synaptic active zones in *Drosophila*. *Neuron* 49, 833-844.
 - Wang, X., Kibschull, M., Laue, M.M., Lichte, B., Petrasch-Parwez, E., and Kilimann, M.W. (1999). Aczonin, a 550-kD putative scaffolding protein of presynaptic active zones, shares homology regions with Rim and Bassoon and binds profilin. *J Cell Biol* 147, 151-162.
 - Wang, Y., Liu, X., Biederer, T., and Sudhof, T.C. (2002). A family of RIM-binding proteins regulated by alternative splicing: Implications for the genesis of synaptic active zones. *Proc Natl Acad Sci U S A* 99, 14464-14469.
 - Wang, Y., Okamoto, M., Schmitz, F., Hofmann, K., and Sudhof, T.C. (1997). Rim is a putative Rab3 effector in regulating synaptic-vesicle fusion. *Nature* 388, 593-598.
 - Wierenga, C.J., Ibata, K., and Turrigiano, G.G. (2005). Postsynaptic expression of homeostatic plasticity at neocortical synapses. *J Neurosci* 25, 2895-2905.
 - Wierenga, C.J., Walsh, M.F., and Turrigiano, G.G. (2006). Temporal regulation of the expression locus of homeostatic plasticity. *J Neurophysiol* 96, 2127-2133.
 - Willeumier, K., Pulst, S.M., and Schweizer, F.E. (2006). Proteasome inhibition triggers activity-dependent increase in the size of the recycling vesicle pool in cultured hippocampal neurons. *J Neurosci* 26, 11333-11341.

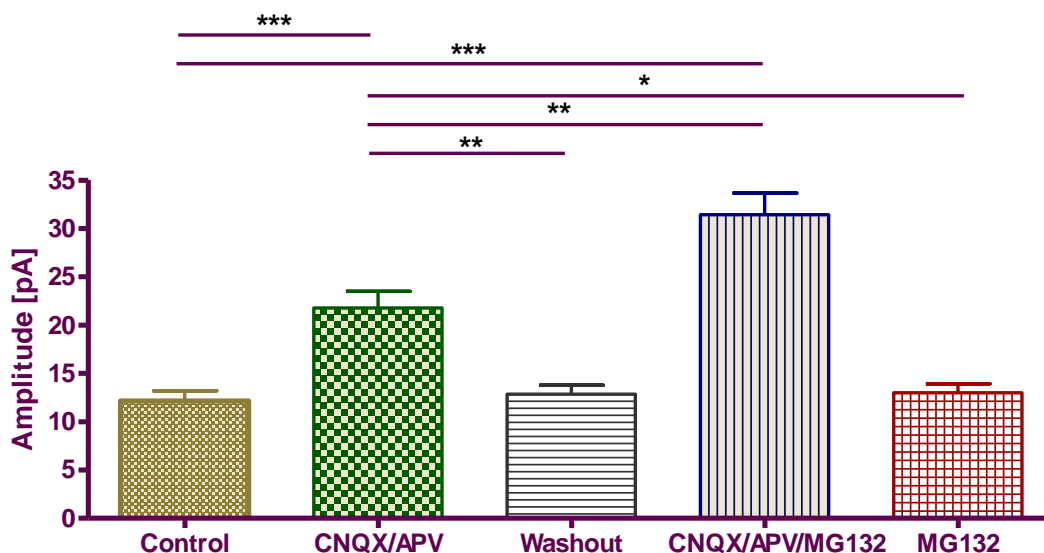
- Wilson, N.R., Kang, J., Hueske, E.V., Leung, T., Varoqui, H., Murnick, J.G., Erickson, J.D., and Liu, G. (2005). Presynaptic regulation of quantal size by the vesicular glutamate transporter VGLUT1. *J Neurosci* 25, 6221-6234.
- Wyszynski, M., Kim, E., Dunah, A.W., Passafaro, M., Valtschanoff, J.G., Serrapages, C., Streuli, M., Weinberg, R.J., and Sheng, M. (2002). Interaction between GRIP and liprin-alpha/SYD2 is required for AMPA receptor targeting. *Neuron* 34, 39-52.
- Zhai, R.G., and Bellen, H.J. (2004). The architecture of the active zone in the presynaptic nerve terminal. *Physiology (Bethesda)* 19, 262-270.
- Zhai, R.G., Vardinon-Friedman, H., Cases-Langhoff, C., Becker, B., Gundelfinger, E.D., Ziv, N.E., and Garner, C.C. (2001). Assembling the presynaptic active zone: a characterization of an active one precursor vesicle. *Neuron* 29, 131-143.
- Zhao, Y., Hegde, A.N., and Martin, K.C. (2003). The ubiquitin proteasome system functions as an inhibitory constraint on synaptic strengthening. *Curr Biol* 13, 887-898.

6. APPENDIX 1

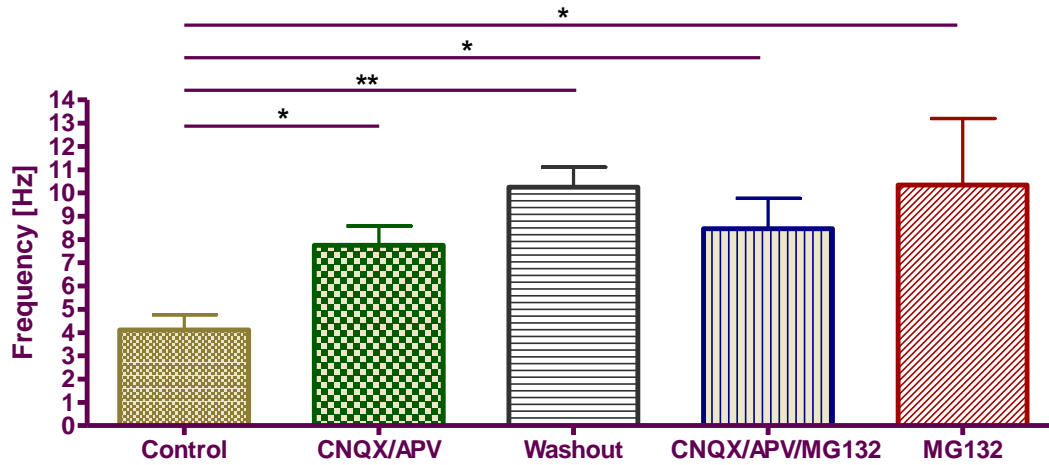
This work has been done by Cornelia Schoene as a part of her Diploma thesis (2009). Similar experimental conditions were used as in the present Ph.D. thesis (see page 35).



Supplementary Fig. S1. Quantification of mEPSC amplitudes (A) and frequencies (B) of cortical cultures in control conditions and after activity deprivation with CNQX/APV. All data were obtained from sister cultures of the same preparation. Different cell densities were analyzed: HD: 300.000 cells/ well, LD: 100.000 cells/well. A significant increase in frequency could be seen in activity deprived neurons at DIV21 (data pooled from 19 to 22 DIV) only for LD cultures (Mean frequency = 7.7 ± 0.8 Hz, $n = 13$) compared to controls (4.2 ± 0.6 Hz, $n = 14$), whereas HD cultures of the same age did not change their frequencies (CNQX/APV: 9.6 ± 2 Hz, control: 9.6 ± 2 Hz, $n = 8$ each). HD cultures show a tendency to increase their frequencies after treatment with CNQX/APV (7.2 ± 1.8 Hz) at 16 DIV compared to controls (4.5 ± 0.8 Hz) ($n = 10$ each, $p = 0.2$). In all conditions, amplitudes were increased after CNQX/APV-treatment (** $p < 0.01$, *** $p < 0.001$, t-test).



Supplementary Fig. S2. Quantification of mEPSC amplitudes of five experimental groups: (from left to right $n = 19, 17, 8, 13, 8$) Treatment for two days with CNQX/APV leads to a significant increase in mEPSP amplitudes compared to untreated controls. This was further increased by addition of proteasome inhibitor MG132 for the last 6 hours of treatment. Effects of CNQX/APV-treatment can be reversed by 2 days washing out with normal media. MG132 alone did not affect mEPSC amplitudes (** $p < 0.01$, *** $p < 0.001$, one-way ANOVA followed by Bonferoni post test).



Supplementary Fig. S3. Mean mEPSC frequencies of five experimental groups: Control (n = 14); CNQX/APV (n = 13); Washout (n = 6); CNQX/APV/MG132 (n = 13); MG132 (n = 6); All treatments lead to a significant increase in frequency. Highest and lowest values of each group were excluded to reduce standard deviation. (** p < 0.01, * p < 0.05, Kruskal-Wallis test followed by Dunn's Multiple Comparisons test).

7. Abbreviations

Abp1	Actin/Dynamin-binding protein 1
AMPA	alpha-amino-3-hydroxy-5-methyl-isoxasole-4-propionic acid
AP	action potential
AZ	active zone
BRP	bruchpilot
Bsn	Bassoon
Bsn/Pclo dMut	Bassoon/Piccolo double mutant
CAMKII	Ca ²⁺ - Calmodulin dependent kinase II
CaMKII	Ca ²⁺ /calmodulin-dependent protein kinases
CASK	Ca ²⁺ /calmodulin-dependent serine protein kinases
CAST	cytomatrix at the active zone associated structural protein
CAZ	cytomatrix of the active zone
CC	coiled-coiled domain
CNQX	6-Cyano-7-nitroquinoxaline-2,3-dione disodium
CNS	central nervous system
CREB	cAMP response element binding
CtBP	C-terminal binding protein
CTRL	Control
D-AP5	D-(-)-2-Amino-5-phosphonopentanoic acid
Div	Day in vitro
DLS	Dynein light chain
DNA	Deoxyribonucleic acid
dSV	docked synaptic vesicles
EM	electron microscope
ERC	
ERK	Extracellular Signal-Regulated Kinase
FCS	fetal calf serum
GABA	gamma-aminobutyric-acid
GKAP	guanylate kinase-associated protein
GluR1	Glutamate receptor 1
GluR2	Glutamate receptor 2
GRIP	glutamate receptor interacting protein
HDACs	histone deacetylases

ICC	immunocytochemistry
IHC	inner hair cell
KIF1A	kinesin-family member 1A
LAR-RPTP	LAR family of receptor protein tyrosine phosphatase
LTD	long-term depression
LTP	long-term potentiation
MALS	mammalian LIN-seven protein
MAP2	microtubule-associated protein 2
MAPK	Mitogen-Activated Protein Kinase
ME-MRI	manganese-enhanced magnetic resonance imaging
mEPSC	miniature excitatory postsynaptic current
NMDA	N-methyl-D-aspartate
NMJ	neuromuscular junction
PBH	Piccolo-Bassoon homology domain
PBS	Phosphate-buffered saline
Pclo	Piccolo
PCR	polymerase chain reaction
PKA	protein kinase A
PKA	protein kinase A
PRA1	Prenylated Rab acceptor protein 1
ProSAP	proline-rich synapse associated protein
PSD	postsynaptic density
PTV	Piccolo-Bassoon transport vesicle
PTX	Picrotoxin
PVDF	polyvinylidene fluoride
RIM	Rab3-interacting molecule
RNA	Ribonucleic acid
RRP	readily releasable pool
RT-PCR	reverse transcriptase- polymerase chain reaction
SAP97	synapse associated protein 97
SAPAP	Synapse-Associated Protein 90/Postsynaptic Density-95-Associated Protein
SDS-PAGE	sodium dodecyl sulphate polyacrylamide gel electrophoresis
SEM	standard error of the mean
SNAP-25	synaptosomal-associated protein of 25 kDa
SNARE	soluble N-ethylmaleimid-sensitive factor attachment protein receptor
SV	synaptic vesicle

Syd-2	synapse-defective-2
TTX	tetrodotoxin
UPS	ubiquitin-proteasome system
VAMP2	vesicle-associated membrane protein 2
VGLUT	Vesicular glutamate transporter
VIAAT	Vesicular Inhibitory Amino Acid Transporter
WB	Western Blot
WT	wild type

8. Curriculum Vitae

Name: Vesna
Family name: Lazarevic
Date of Birth: Jun 2nd 1978
Place of Birth: Belgrade, Serbia
Nationality: Serbian
Parents: Dusan Lazarevic
Milosava Lazarevic

Education:

2006 - 2009 Doctoral theses. Otto-von-Guericke University –Leibniz
Institute for Neurobiology, Magdeburg, Germany.

Sept.2005 - Dec.2005. Practical training at Leibniz Institute for Neurobiology,
Magdeburg, Germany.

1997/98 - 2004/05 Faculty of Biology
Department for Molecular Biology and Physiology
Group of Experimental Biomedicine
University of Belgrade, Belgrade, Serbia

2004 - 2005 Diploma study at the Institute of Immunology and
Virology "Torlak", Belgrade

1993 -1997 High School, Natural/Mathematical Course

October, 20th 2009, Magdeburg

Scientific publications:

Fejtova, A., Davydova, D., Bischof, F., **Lazarevic, V.**, Altmann, W.D., Romorini, S., Schone, C., Zuschratter, W., Kreutz, M.R., Garner, C.C., Ziv N.E. and Gundelfinger, E.D. (2009) Dynein light chain regulates axonal trafficking and synaptic levels of Bassoon. *J Cell Biol* 185, 341-355.

9. Erklärung zur eigenständigen Abfassung der Arbeit

Hiermit erkläre ich, Vesna Lazarevic, dass ich die von mir eingereichte Dissertation zum dem Thema

“Mechanisms of assembly and activity-dependent remodelling of the presynaptic cytomatrix at the active zone”

selbständig verfasst, nicht schon als Dissertation verwendet habe und die benutzen Hilfsmittel und Quellen vollständig angegeben wurden.

Weiterhin erkläre ich, dass ich weder diese noch eine andere Arbeit zur Erlangung des akademischen Grades doctor rerum naturalium (Dr. rer. nat.) an anderen Einrichtungen eingereicht habe.

Magdeburg, 20.10.2009.

Unterschrift

